

ECOLE POLYTECHNIQUE
Master 1
PASQUINELLI Irene

RAPPORT DE STAGE DE RECHERCHE

*Cutting sequences in
Veech surfaces*

NON CONFIDENTIEL
PUBLICATION

Option : Département de MATHEMATIQUES

Champ de l'option : Systèmes Dynamiques

Directeur de l'option : Charles Favre

Directeur de stage : Corinna Ulcigrai

Dates du stage : 08 avril – 31 août 2013

Nom et adresse de l'organisme :

University of Bristol

School of mathematics

University Walk

BS8 1TW

Bristol

United Kingdom

Abstract

A cutting sequence is a symbolic coding of a linear trajectory on a translation surface corresponding to the sequence of sides hit in a polygonal representation of the surface.

We characterize cutting sequences in a regular hexagon with opposite sides identified by translations exploiting the same procedure used by Smillie and Ulcigrai in [SU11] for the regular octagon.

In the case of the square, cutting sequences are the well known Sturmian sequences. We remark the differences between the procedure used in the case of the square and the one used in the cases of the regular hexagon and regular octagon. We also show how to adapt the latter to work also in the case of the square, giving a new characterization for this case.

We also show how to create a dictionary to pass from the symbolic coding with respect to the hexagon to the symbolic coding with respect to the parallelogram representing it in the space of flat tori.

Finally we consider the Bouw-Möller surfaces $\mathcal{M}(3,4)$ and $\mathcal{M}(4,3)$ and we use their semi-regular polygons representations to prove our main result, which is a theorem analogous to the central step used to characterize cutting sequences in the previous cases.

Résumé

Une suite de codage est un code symbolique d'une trajectoire linéaire dans une surface de translation et elle correspond à la succession des côtés croisés dans une représentation polygonale de la surface.

Nous caractérisons les suites de codage dans un hexagone régulier avec côtés parallèles identifiés par des translations en utilisant la même procédure que celle présentée par Smillie et Ulcigrai dans [SU11].

Dans le cas du carré, les suites de codage sont les bien connues suites de Sturm. Nous montrons les différences entre la procédure utilisée dans le cas du carré et celle utilisée pour les cas de l'hexagone régulier et de l'octogone régulier. Nous montrons aussi comment adapter la deuxième pour l'appliquer au cas du carré aussi et nous donnons donc une nouvelle caractérisation dans ce cas.

Nous montrons aussi comment créer un dictionnaire pour passer du code symbolique lié à l'hexagone à celui lié au parallélogramme qui représente l'hexagone dans l'espace des tores plats.

Enfin nous considérons les surfaces de Bouw-Möller $\mathcal{M}(3,4)$ et $\mathcal{M}(4,3)$ et nous utilisons ses représentations en polygones semi-réguliers pour démontrer notre résultat principal, qui est un théorème analogue à l'étape centrale de la démonstration de la caractérisation des suites de codage dans les cas précédents.

Contents

1	Cutting sequences for the hexagon	6
1.1	Main definitions	6
1.1.1	Transition diagrams	6
1.1.2	Derivation	8
1.1.3	Veech group	10
1.2	Necessary condition	12
1.2.1	Veech element	12
1.2.2	Statement	15
1.2.3	Proof	16
1.3	Farey map	19
1.3.1	Definition	19
1.3.2	Hexagon Farey expansion	20
1.3.3	Direction recognition	20
1.4	Characterization	21
1.5	Teichmüller disk	24
1.5.1	Marked translation surfaces and its actions	24
1.5.2	Teichmüller geodesics and hexagonal tiling	27
1.5.3	Teichmüller cutting sequences	29
2	Hexagon vs square	31
2.1	Derivations in the square	31
2.1.1	Series derivation	31
2.1.2	Where sandwich derivation fails	31
2.1.3	How sandwich derivation can work	32
2.2	Hexagon as a flat torus	34
2.2.1	Space of flat tori	34
2.2.2	Dictionary	35
2.2.3	Relations	37
3	Cutting sequences for a Bouw-Möller surface	37
3.1	Two representations of the surface	38
3.2	Transition diagrams	41
3.3	Derivation	43
3.4	Veech element	44
3.5	Future works	47
	References	49

Introduction

This work deals with cutting sequences of linear trajectories in translation surfaces.

A translation surface, precisely defined in Paragraph 1.1.3, is obtained by polygons, gluing pairs of parallel sides by translations. In the representation of the surface by polygons, linear trajectories are nothing else but straight lines in the interior of the polygons. When the line hits one side, it comes out from the corresponding point of the glued side.

We can code trajectories by labelling each pair of identified sides with a letter and by recording the sequence of letters of sides hit by the trajectory. Supposing a trajectory does not hit the vertices, this gives us a bi-infinite sequence of letters in the alphabet we are using. This is called the *cutting sequence* of the trajectory.

We want to try to understand which information about the trajectory we can recover from the cutting sequence. For example, can we characterize the cutting sequences in the space of bi-infinite sequences? In other words, given a bi-infinite sequence is it possible to find out whether it is a cutting sequence of a certain trajectory or not? And if it is, can we recover the direction of such trajectory?

The problem has already been studied in many cases. The first well known and long studied one is a square with opposite sides identified, treated for example by Caroline Series in [Ser85a]. Since the square tessellates the plane, the problem is equivalent to coding straight lines in the plane with respect to a horizontal and vertical grid. The cutting sequences obtained in this way are called *Sturmian sequences* and appear in various areas of mathematics.

The second case studied was the one of the regular octagon, together with other regular $2n$ -gons for $n \geq 4$, described by John Smillie and Corinna Ulcigrai in [SU11]. There, they explain that in this case, characterizing cutting sequences is a bit more complicated but still possible, in a similar way to Sturmian sequences.

The third case is the one of regular pentagon and in general regular odd-gons. In this case, since there are not anymore opposite parallel sides to glue, Veech originally used two copies of them glued together to build a translation surface. In [Dav13] Diana Davis analysed this case and showed that the same procedure as Smillie and Ulcigrai can be applied for the double regular pentagon and the general case of double regular odd-gons.

The first part of my work, described in Section 1, was to consider the case of the hexagon, ignored until now because by gluing the opposite parallel sides we obtain a torus, and hence the same kind of surface as in the case of the square. This case turns out to be exactly as the case of the octagon and in the first part of this work we explain the procedure used first in [SU11], applying it to the case of the hexagon.

In the first part 2.1 of the second section of this work, we compare the methods used for the square and for the hexagon. Even if the general method is the same, there is a slight difference between definitions and tools used in the case

of the hexagon (and octagon and pentagon) and the one used in [Ser85a] for the square. We analyse the differences between the two procedures and we show that the first method can be adapted to work also for the square and give an other characterization of Sturmian sequences.

Then, in the second part of the second section (see 2.2) since the hexagon and the square in the space of flat tori are not the same surface, we explain the link between symbolic coding for the hexagon and the symbolic coding for the correspondent parallelogram in the space of flat tori.

In the third part of this work, described in Section 3 we analyse a particular surface of a new family of translation surfaces, the Bouw-Möller surfaces, introduced by Irene Bouw and Martin Möller in [BM10] and described by Pat Hooper in [Hoo12] as semi-regular polygons glued together.

The problem of studying cutting sequences on these surfaces is still open, although some first results are obtained by Diana Davis in [Dav14].

Bouw-Möller surfaces share an important property with surfaces obtained by gluing regular polygons: they are all Veech surfaces. The idea is that a Veech surface is a translation surface which has plenty of affine symmetries. More precisely, this means that it is a translation surface whose Veech group (defined in 1.1.3) is a lattice in $SL(2, \mathbb{R})$. In particular, this means that the quotient of the space of deformations under its action is a hyperbolic surface with finite area.

The general idea to characterize cutting sequences is to define a combinatorial operation on words called *derivation* and show that cutting sequence are infinitely derivable. The proof is based on the fact that we can cut and paste the original polygon to obtain a new presentation as a sheared polygon and show that the cutting sequence of the same trajectory with respect to the new sides is exactly the derived sequence of the original sequence. By sending the sheared polygon back in the original one with a shear, we obtain a new trajectory. We can repeat the argument and find out that the derived sequence of a cutting sequence is still a cutting sequence and hence cutting sequences are infinitely derivable.

Finally, it is well known that the characterization of Sturmian sequences is intimately connected with the geodesic flow on the modular surface, as explained by Caroline Series in [Ser85b]. Similarly, in the case of the octagon and of the pentagon, as well as in the case of the hexagon, the characterization is connected with the Teichmüller geodesic flow on the Teichmüller disk, as shown from Smillie and Ulcigrai in [SU10] for the octagon and here in Paragraph 1.5 for the hexagon.

This and the brief outline of the central observation, show that we deeply use the Veech group and hence the property of being a Veech surface. This is why the case of Bouw-Möller surfaces can be treated similarly to the previous ones.

1 Cutting sequences for the hexagon

1.1 Main definitions

Following [SU11] we can provide the same construction for the hexagon. Consider the hexagon E centred in the origin of the axis and with one edge parallel to the horizontal axis. We now label the edges as follow: let's call A the horizontal sides and continue labelling B and C clockwise. By gluing the opposite parallel pairs of sides by translations, we obtain a Veech surface that we will call S_E , of genus 1, with two fake singularities given by the vertices. Let us consider now a linear trajectory in the surface. Obviously, it projects to a straight line in the hexagon. For simplicity, we suppose to have just bi-infinite trajectories, never hitting the fake singularities, which means that our trajectories never hit vertices of the hexagon.

We can now *code* the trajectory by writing down the letters of the sides hit by the trajectory. If we consider then the set of all labels as an alphabet $\mathcal{A} = \{A, B, C\}$, we have that the sequence of labels is a bi-infinite word in the alphabet, that we will call *cutting sequence* and denote as $c(\tau)$ where τ is the trajectory.

1.1.1 Transition diagrams

We try now to study the cutting sequences of such a surface.

As for the octagon, up to applying a rotation of angle π we can consider $\theta \in [0, \pi]$ because this leaves the labels unchanged.

The symmetries of the hexagon suggests that we can divide $[0, \pi]$ in the sectors $\Sigma_i = [\frac{i\pi}{6}, \frac{(i+1)\pi}{6}]$ for $i = 0, \dots, 5$ and consider the element of D_6 which sends the sector Σ_i back in Σ_0 . They are expressed by the following matrices:

$$\begin{aligned} \nu_0 &= \text{Id}, & \nu_1 &= \rho_{\frac{\pi}{6}} \circ r_1 \circ \rho_{-\frac{\pi}{6}} = \begin{pmatrix} \frac{1}{2} & \frac{\sqrt{3}}{2} \\ \frac{\sqrt{3}}{2} & -\frac{1}{2} \end{pmatrix}, \\ \nu_2 &= \rho_{-\frac{\pi}{3}} = \begin{pmatrix} \frac{1}{2} & \frac{\sqrt{3}}{2} \\ -\frac{\sqrt{3}}{2} & \frac{1}{2} \end{pmatrix}, & \nu_3 &= \rho_{-\frac{\pi}{6}} \circ r_2 \circ \rho_{\frac{\pi}{6}} = \begin{pmatrix} -\frac{1}{2} & \frac{\sqrt{3}}{2} \\ \frac{\sqrt{3}}{2} & \frac{1}{2} \end{pmatrix}, \\ \nu_4 &= \rho_{-\frac{2\pi}{3}} = \begin{pmatrix} -\frac{1}{2} & \frac{\sqrt{3}}{2} \\ -\frac{\sqrt{3}}{2} & -\frac{1}{2} \end{pmatrix}, & \nu_5 &= r_2 = \begin{pmatrix} -1 & 0 \\ 0 & 1 \end{pmatrix}. \end{aligned}$$

Note that we call ρ_θ the counter-clockwise rotation of angle θ and we call r_1 and r_2 the reflections through respectively the horizontal axis and the vertical axis.

They act on the labels (and hence on the cutting sequences) by *permuting* the labels and we can write explicitly the permutations that they induce:

$$\begin{array}{ll}
\pi_0 = \text{Id}, & \pi_1 = (AC), \\
\pi_2 = (ABC), & \pi_3 = (BA), \\
\pi_4 = (ACB), & \pi_5 = (BC).
\end{array}$$

We want now to try to understand which words in the alphabet can be cutting sequences and which ones cannot.

First of all, we check which transitions can occur in a cutting sequence, i.e. which couple of letters can be found one after the other in a cutting sequence.

What we do is to fix a sector, and to try to understand (and represent in a graph) where else can a trajectory in that range of directions go, if it just hit a certain side. As we saw, it is enough to study transitions for trajectories with direction in Σ_0 because the others will be obtained by permuting the labels.

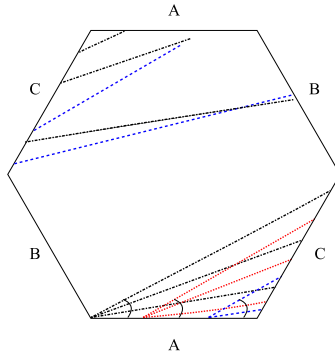


Figure 1: Diagram \mathcal{D}_0

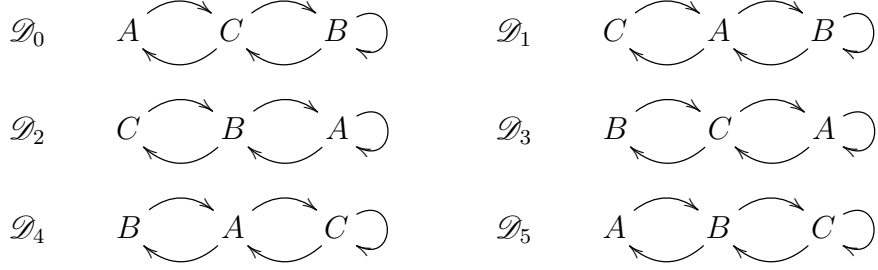
To describe them, we construct the related transition diagram \mathcal{D}_0 . A cutting sequence will then give a bi-infinite path in the diagram.

We start from the bottom horizontal side labelled A and we see in Figure 1 that all possible trajectories in a direction in Σ_0 necessarily go through C and so on, obtaining the following diagram.



Similarly, we can construct all the diagrams for the other sectors of directions by applying the permutations on the labels induced by the action on the labels of the previous matrices.

The diagrams become hence:



Remark 1.1. Since each matrix induces a permutation of labels as we just saw, we also have an action of each π_i on the space of bi-infinite words $\mathcal{A}^{\mathbb{Z}}$. Moreover, when passing to cutting sequences, this action commutes with the action of the corresponding matrices on the trajectory. In fact, for each $0 \leq k \leq 5$ we have

$$c(\nu_k \tau) = \pi_k \cdot c(\tau).$$

By mapping a trajectory in direction $\theta \in [0, \pi]$ to Σ_0 with one of the ν_i 's and up to permuting the labels which appear in the cutting sequence, we can assume that $\theta \in [0, \frac{\pi}{6}]$.

We will often need to consider a trajectory in some direction $\theta \in [0, \pi]$ and *send it back* to a trajectory with direction in Σ_0 in order to simplify exposition and prove our results using just our first sector. We will then often consider the *normal form* of a trajectory defined by

Definition 1.2. The normal form of a trajectory in direction $\theta \in \Sigma_k$ is the trajectory

$$n(\tau) = \nu_k \tau.$$

1.1.2 Derivation

Our aim is to give conditions under which a word in the alphabet is or is not a cutting sequence. First of all we can see that since we constructed transition diagrams describing all possible transitions in a cutting sequence, we have that all cutting sequences can be described as a path in one of the diagrams \mathcal{D}_i .

To state this more precisely, we need to define that

Definition 1.3. A word in the alphabet is admissible if it describes a bi-infinite path in one of the \mathcal{D}_i , i.e. if the transitions appearing in the word are all allowed in one of the diagrams. In that case we will say that the word is admissible in the diagram i .

Therefore, a necessary condition for cutting sequences is the following:

Lemma 1.4. *If $w \in \mathcal{A}^{\mathbb{Z}}$ is a cutting sequence, it is admissible in some diagram \mathcal{D}_k .*

In order to get a characterization, one needs a stronger condition (see Proposition 1.18 in the next section). In order to define it, let us first introduce a combinatorial operation on admissible words.

Definition 1.5. Given a letter L in a word $w \in \mathcal{A}^{\mathbb{Z}}$, we say it is sandwiched if the previous and the following letters are the same letter L' .

The operation on words is hence:

Definition 1.6. If $w \in \mathcal{A}^{\mathbb{Z}}$ is an admissible word, its derived sequence $w' \in \mathcal{A}^{\mathbb{Z}}$ is the word obtained from w keeping all sandwiched letters and dropping the others.

Remark 1.7. The condition of admissibility for w is necessary for having a bi-infinite word. In fact, one can easily check that starting from every point of a diagram and considering all possible paths, after a finite number of steps one continues to meet new sandwiched letters. Bi-infinite admissible sequences will then give bi-infinite derived sequences.

For cutting sequences the admissibility condition is automatically satisfied.

Remark 1.8. It will also be useful to notice that the property of being sandwiched for letters is invariant with respect to permutations. Precisely:

$$(\pi \cdot w)' = \pi \cdot w'$$

where π is a permutation.

We also have a similar construction of a *normal form* as in 1.2 for a certain subset of sequences. In fact we can define

Definition 1.9. If w is a word admissible in just one diagram \mathcal{D}_k for a certain $k \in \{0, \dots, 5\}$, the normal form of w is the word $n(w) = \pi_k \cdot w$.

The concept of derivation on sequences allows us to describe an important subset of sequences:

Definition 1.10. $w \in \mathcal{A}^{\mathbb{Z}}$ is derivable if it is admissible and its derived sequence is still admissible.

And recursively we have also

Definition 1.11. $w \in \mathcal{A}^{\mathbb{Z}}$ is infinitely derivable if it is derivable and deriving n times we obtain always a derivable sequence, for all n .

As we will state precisely and prove in the following section, all cutting sequences are infinitely derivable. We will prove that the derived sequence of a cutting sequence is again a cutting sequence.

1.1.3 Veech group

What we still need in order to state and prove the condition is to recall the definition of the affine automorphism group and of the Veech group. Following the novel approach of [SU11], we will allow orientation-reversing affine automorphisms.

We recall following [Mas06] that a translation surface is a finite union (just one in this case) of polygons with identifications of pairs of parallel sides such that

- the boundaries of the polygons are oriented so that the polygon lies to the left;
- Each side is glued to another parallel side of same length by translation so that the two sides have opposite orientations.

Using this definition our surface S_E is naturally a translation surface.

Equivalently, a translation surface is a surface S with a set of singularities Σ such that $S \setminus \Sigma$ is covered by an atlas $\{U_\alpha, \phi_\alpha\}$ for which the changes of charts on the intersections are translations:

$$\phi_\alpha \phi_\beta^{-1}(v) = v + c.$$

The singular points are cone singularities which possibly arises from the vertices of the polygons (in our case they are just fake singularities). The surface inherits a flat metric which allows us to talk about trajectories, which are geodesics with respect to the metric.

Using this second definition, we can state how to deform a translation surface:

Definition 1.12. Given $\eta \in GL(2, \mathbb{R})$ the deformation of a translation surface S by η is the translation surface S' obtained by applying η to the images under the charts, which means considering the atlas $\{U_\alpha, \eta \cdot \phi_\alpha\}$ and fixing the singularities.

If we use the first definition, we can consider the surface obtained by gluing the images of the sides of the polygons after applying η to the polygons themselves.

A deformation of S by η is hence the natural application

$$\Phi_\eta: S \rightarrow S' = \eta \cdot S$$

and with abuse of notations we will sometimes refer to such a map by writing deformation of S .

Remark 1.13. Obviously, it sends linear trajectories τ in S to linear trajectories $\eta\tau$ in S' and the set of singularities in the set of singularities.

We just explained how to associate a matrix in $GL(2, \mathbb{R})$ to a deformation of S which is a particular affine diffeomorphism:

Definition 1.14. An affine diffeomorphism Ψ between S and S' translation surfaces is a homeomorphism which preserve the set of singularities i.e. sends Σ in Σ' and outside is a diffeomorphism such that the derivative $D\Psi_p$ at the point $p \in S$ between the tangent spaces does not depend on p .

In fact the derivative of the deformation Φ_η is the matrix η in every point of $S \setminus \Sigma$.

Conversely, to each affine diffeomorphism, we can associate, by a map that we call V , a matrix in $GL(2, \mathbb{R})$ as the derivative $D\Psi$.

We will say that S and S' are affinely equivalent if it exists an affine diffeomorphism between them, isometric if it exists such affine diffeomorphism and its derivative is in $O(2)$ and translation equivalent if there exists such an affine diffeomorphism Υ and its derivative is the identity. In the last case, the map Υ , up to cutting the polygons composing S in smaller pieces, can be defined locally on each piece as a translation in order to give out the polygons composing S' .

In the case $S = S'$ the affine diffeomorphisms are called affine automorphisms and form a group we will call $\text{Aff}(S)$.

Let us now consider V that is called the *Veech homomorphism* for $S = S'$

$$\begin{aligned} V: \text{Aff}(S) &\rightarrow GL(2, \mathbb{R}) \\ \Psi &\mapsto D\Psi. \end{aligned}$$

Naturally the image is in $SL_\pm(2, \mathbb{R})$, which is the subgroup of matrices with determinant ± 1 and we will call such image the *Veech group* of S and write $V(S)$. Practically speaking it is the set of derivatives of affine automorphisms of a surface.

Traditionally, the Veech group is considered to be the intersection of such a group with $SL(2, \mathbb{R})$ i.e. the orientation-preserving elements that we will call $V^+(S)$. Moreover, sometimes it is considered to be the projection of such a group in $PSL(2, \mathbb{R})$ which we will call $V_P^+(S)$ while the projection in $PGL(2, \mathbb{R})$ will be denoted by $V_P(S)$.

The Kernel of V is the set of translation equivalences of S and it is trivial if and only if given the derivative, the affine automorphism is automatically determined because injectivity guarantees that we can't have two preimages. In that case the most classical example of affine automorphism is hence the unique one and it can be described as follow: given S as identified polygons and its derivative η we can compose the canonical map described above $\Phi_\eta: S \rightarrow \eta \cdot S$ with a translation equivalence $\Upsilon: \eta \cdot S \rightarrow S$ uniquely determined by the derivative if the kernel of V is trivial. We obtain an affine equivalence $\Psi_\eta: S \rightarrow S$.

An other useful way to describe the Veech group of our surface S_E is to consider the map

$$\begin{aligned}
h: SL(2, \mathbb{R}) &\rightarrow SL(2, \mathbb{R}) \cdot S_E \\
A &\mapsto A \cdot S_E.
\end{aligned}$$

It's kernel is the set $V(S_E) = \{A: A \cdot S_E \doteq S_E\}$ where " \doteq " means that the two surfaces can be obtained one from the other by a cut and paste map which actually is a translation equivalence. This means that each time we apply an element of the Veech group to the hexagon we will always have a cut and paste map which sends the new polygon back to the previous one and hence this shows the equivalence with the previous definition.

Veech proved in [Vee89] that the orientation-preserving Veech group of each translation surface obtained by gluing regular polygons is a lattice in $SL(2, \mathbb{R})$ which naturally means that our Veech group $V(S)$ is a lattice in $SL_{\pm}(2, \mathbb{R})$. Surfaces satisfying such property are called Veech surfaces.

But we can say something more about the structure of the Veech group of our surface. First of all we have that each element of the dihedral group $\eta \in D_6$ determines an affine automorphism as explained before $\Psi_{\eta}: S_E \rightarrow S_E$ whose derivative is exactly η which means that the dihedral group is a subgroup of the Veech group. In particular, we have the reflection with respect to the horizontal axis and the reflection with respect to the straight line forming angle $\frac{\pi}{6}$ with the horizontal axis:

$$\alpha = \begin{pmatrix} 1 & 0 \\ 0 & -1 \end{pmatrix} \quad \beta = \begin{pmatrix} \frac{1}{2} & \frac{\sqrt{3}}{2} \\ \frac{\sqrt{3}}{2} & -\frac{1}{2} \end{pmatrix}$$

and their counterpart as affine automorphisms Ψ_{α} and Ψ_{β} .

By adapting the proofs of the orientation-preserving case exactly as for the octagon in [SU11] we can describe precisely the Veech group for the hexagon and state the following:

Lemma 1.15. *The kernel of V from $\text{Aff}(S_E)$ to $GL(2, \mathbb{R})$ is trivial.*

Moreover, the affine automorphisms group $\text{Aff}(S_E)$ is generated by Ψ_{α} , Ψ_{β} and Ψ_{γ} and hence the Veech group is generated by their derivatives α , β , γ , where $\gamma = \begin{pmatrix} -1 & 2\sqrt{3} \\ 0 & 1 \end{pmatrix}$, the Veech shear described in the next paragraph.

1.2 Necessary condition

1.2.1 Veech element

We will now describe the third generator of the Veech group γ .

We know that if we have a decomposition in cylinders with commensurable moduli, then we can define an affine automorphism with a shear as derivative which acts as a multiple of a Dehn twist on each cylinder.

The best thing is to show it on an example. Let us consider a rectangle with two parallel sides identified, say the vertical sides. Its modulus, which we call m , is the ratio $\frac{\text{height}}{\text{width}}$ and is the slope of the diagonal. If $\mu = \frac{1}{m}$ we now apply to the rectangular representation the shear $\begin{pmatrix} 1 & \mu \\ 0 & 1 \end{pmatrix}$. The horizontal lines remain horizontal, while the vertical ones are sent in lines of slope $\frac{1}{\mu} = m$, which means that the new sides are the horizontal side and the diagonal. It is clear that the diagonal is somehow the geodesic which goes along both the previous ones and hence we can describe the related affine automorphism ψ (with derivative the shear) as in Figure 2, by "twisting" the two extremities of the cylinder.

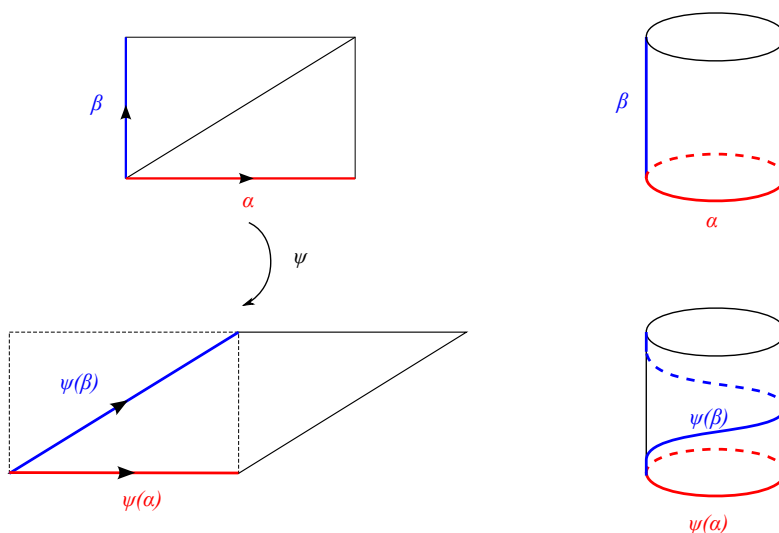


Figure 2: Dehn twist on a cylinder

When we have more than one cylinder, on each cylinder we know how to do a Dehn twist and obviously a multiple of it. Suppose hence that $S = \cup_i C_i$ and on each C_i we know how to apply $\psi_i^{n_i}$, for ψ_i basic Dehn twist and $n_i \in \mathbb{N}$. We define the affine automorphism $\psi(x) = \psi_i^{n_i}(x)$ if $x \in C_i$ and n_i is determined by the condition of being an affine automorphism. In fact it is equivalent to say that $D\psi_i = A$, a certain matrix independent on i and since $D(\psi_i^{n_i}) = \begin{pmatrix} 1 & \mu_i^{n_i} \\ 0 & 1 \end{pmatrix}$, we just need to choose a μ such that $\mu = \mu_i^{n_i} = \mu_j^{n_j}$ for all i, j (and it is possible if the moduli are commensurable) and define ψ such that its derivative is

$$A = \begin{pmatrix} 1 & \mu \\ 0 & 1 \end{pmatrix}.$$

It is independent on i and it is a multiple of the standard Dehn twist on each cylinder. Naturally, the matrix A being the derivative of an affine automorphism is an element of the Veech group.

In the case of the hexagon the corresponding orientation reversing element (i.e. the composition of such an element with the reflection with respect to the vertical axis) is exactly the element γ of the previous section, one of the generators of the Veech group.

In order to find out explicitly that element, first of all we need a decomposition in cylinders of the hexagon.

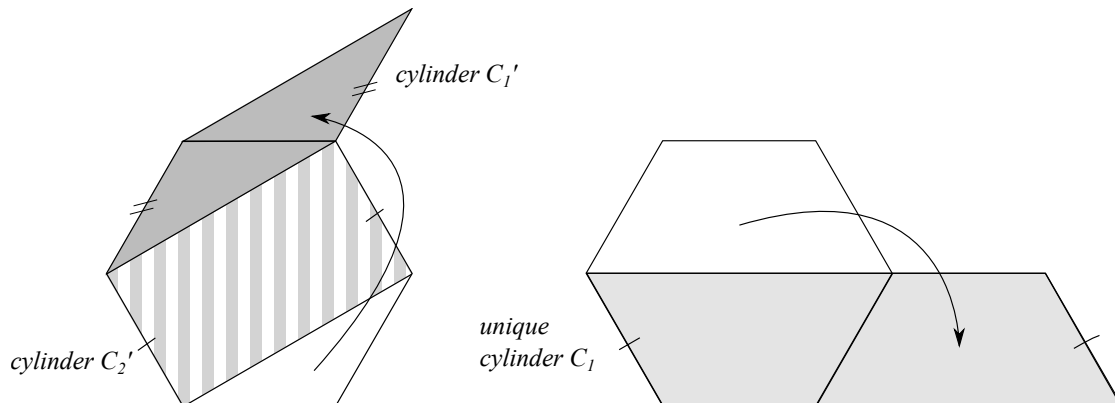


Figure 3: cylinder decompositions

By looking at Figure 3, we find out that we have two possible cylinder decompositions. The two decompositions are in the direction $\theta = 0$ and $\theta = \frac{\pi}{6}$ and we consider the horizontal one. It consists in cutting the hexagon horizontally, and glueing the upper part to the side C , so that we obtain a cylinder which has height $\frac{\sqrt{3}}{2}$ and width 3. This means that its inverse modulus is $\mu = 2\sqrt{3}$. Obviously we don't either have the problem of commensurability and this gives us straightforwardly an affine diffeomorphism Ψ_σ which acts on the cylinder by a Dehn twist fixing horizontal lines, sending vertical lines in lines of slope $\frac{1}{\mu}$ and fixing singularities. Automatically, this gives the element of the Veech group:

$$\sigma = \begin{pmatrix} 1 & 2\sqrt{3} \\ 0 & 1 \end{pmatrix},$$

as derivative of the affine diffeomorphism. The image of such an element is a new (not regular) hexagon $E' = \sigma E$ shown in Figure 4 and by definition of Veech group can be cut and pasted again in the original hexagon E . We call such a cut and paste map, a piecewise translation, by Υ_E . His derivative is obviously the identity and hence the affine automorphism Ψ_σ of the glued surface S_E named before is exactly $\Upsilon_E \circ \sigma$.

In order to simplify the notions that we will see later on, we consider an other element of the Veech group, which acts in the same way as σ but reversing the orientation of the labels. We define then

$$\gamma = \begin{pmatrix} -1 & 2\sqrt{3} \\ 0 & 1 \end{pmatrix} = \sigma \circ r_2$$

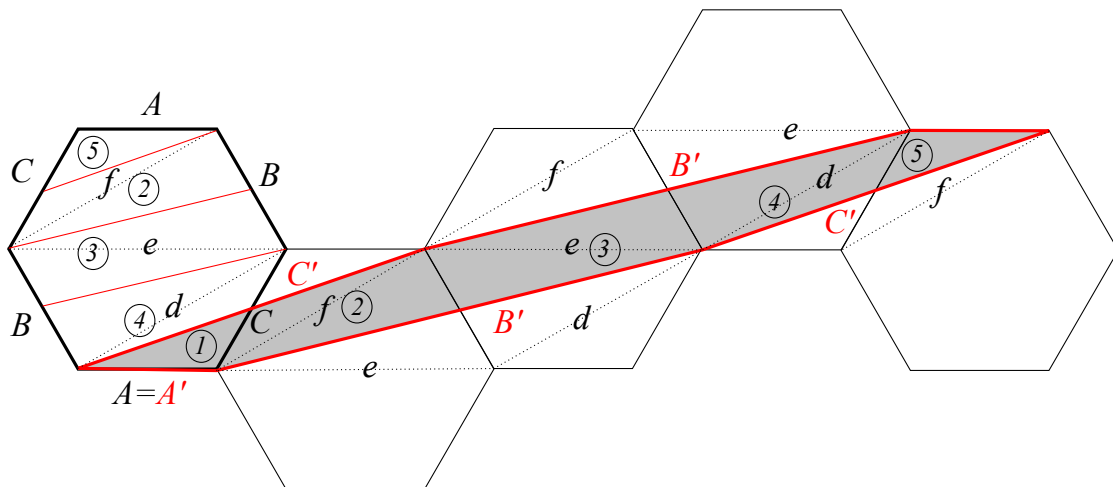


Figure 4: Action of the shear

which means that acting by γ means reflecting the hexagon with respect to the vertical axis (i.e. exchanging the labels B and C , or equivalently reverting the orientation of the labels) and then acting by the shear σ . It is easy to see that γ is an involution because its square is the identity.

1.2.2 Statement

The whole discussion about finding a necessary condition for a sequence in the alphabet for being a cutting sequence is based on a simple proposition, whose proof is purely combinatorial, but has a huge geometrical hidden sense. The condition is

Theorem 1.16. *A cutting sequence is infinitely derivable.*

The proof is very simple using the following:

Proposition 1.17. *The derived sequence of a cutting sequence is again a cutting sequence.*

In fact, if the derived sequence is a cutting sequence, it is admissible in some of the diagrams \mathcal{D}_i and hence by definition the original one is derivable. By repeating this argument, we obtain the infinite derivability.

Our next step will be then to rephrase Proposition 1.17 in a more precise way and prove it.

Proposition 1.18 (Central Proposition). *Given a trajectory τ in direction $\theta \in \Sigma_0$ with cutting sequence $c(\tau)$, let us consider the trajectory $\tau' = \Psi_\gamma \tau$. We have that the cutting sequence of the new trajectory is exactly the derived sequence of the cutting sequence of the old one. It means that*

$$c(\tau') = c(\tau)'$$

Proving the second proposition, 1.18, is enough to obtain the previous one, 1.17.

In fact suppose we have a trajectory τ in direction $\theta \in \Sigma_i$ and call $w = c(\tau)$ its cutting sequence. Using the second proposition we will show that the derived sequence w' is again a cutting sequence of a certain trajectory that will be explicit later. As one immediately sees the problem is in showing that we can somehow pass from trajectories in whatever direction to trajectories in Σ_0 and a similar statement for a different τ' is true. In fact by considering the normal form defined by $n(w) = \nu_i \tau \in \Sigma_0$, we can apply Proposition 1.18 and obtain that

$$c(\Psi_\gamma \nu_i \tau) = c(\nu_i \tau)' = (\pi_i \cdot c(\tau))' = \pi_i \cdot (c(\tau))'$$

where the last inequalities are respectively Remark 1.1 and the invariance of the sandwich property under relabelling. But then we can consider the trajectory $\nu_i^{-1} \Psi_\gamma \nu_i \tau$ and a similar argument gives

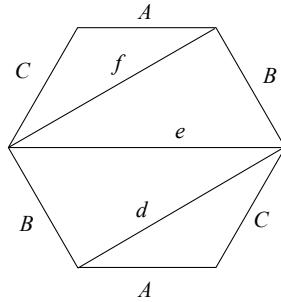
$$\begin{aligned} c(\nu_i^{-1} \Psi_\gamma \nu_i \tau) &= \pi_i^{-1} \cdot c(\Psi_\gamma \nu_i \tau) = \dots \text{previous equalities} \dots = \\ &= \pi_i^{-1} \cdot \pi_i \cdot (c(\tau))' = c(\tau)' = w'. \end{aligned}$$

This means then that the derived sequence of the cutting sequence of a trajectory τ in a direction in the i -th sector is again a cutting sequence and precisely it is the cutting sequence of the trajectory $\nu_i^{-1} \Psi_\gamma \nu_i \tau$.

1.2.3 Proof

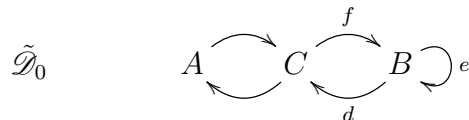
It remains now to prove Proposition 1.18 and we do it immediately.

Proof. We divide the proof in four simpler steps.



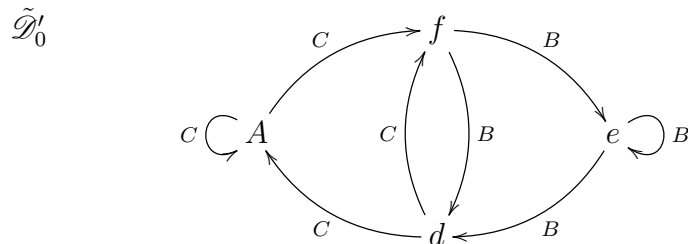
First step: First of all, we mark in the hexagon the diagonals in directions 0 and $\frac{\pi}{6}$ (the auxiliary edges), and label them d, e, f starting from the bottom, as in Figure 1.2.3. If now we consider the cutting sequence of τ , we can record whenever it crosses these diagonals by writing down what we will call the *augmented cutting sequence* $\tilde{c}(\tau) \in \{A, B, C, d, e, f\}^{\mathbb{Z}}$. If we remember that the cutting sequence of a trajectory in direction $\theta \in \Sigma_0$ represents a path in the diagram \mathcal{D}_0 , we can

construct an other diagram $\tilde{\mathcal{D}}_0$ on which the same path will give us the augmented cutting sequence reading both the pointed letters and the labels of the arrows. In fact, we can see that for each transition, we can either cross or not an auxiliary edge and it is always well determined. The new diagram becomes hence:



and it will allow us to determine univocally the augmented cutting sequence using $c(\tau)$.

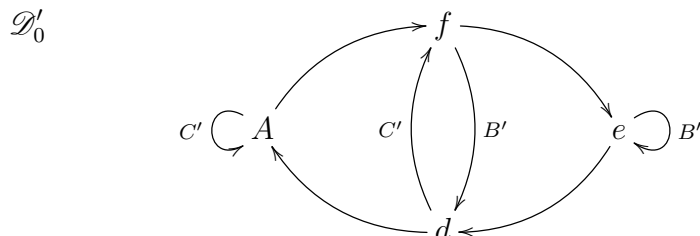
Second step: We now try to interchange the roles of edges and vertices of the new diagram except for A , which is somehow both a normal side and an auxiliary side, since it is a "diagonal" in direction 0. What we mean geometrically is to obtain a code for the trajectory not based on the original sides, but on the auxiliary sides, recording as before the crossings with normal sides. B and C become hence labels of arrows and the diagrams is



The new diagram can determine a new "cutting sequence" representing a path in $\tilde{\mathcal{D}}'_0$ and coding the trajectory with respect to the auxiliary sides. We will call it $\hat{c}(\tau) \in \{A, d, e, f\}^{\mathbb{Z}}$ and is obtained from $\tilde{c}(\tau)$ by erasing B 's and C 's.

Third step: Let us now apply the cut and paste map $\Upsilon_E^{-1} = E'$. As we saw, we obtain a new hexagon and we label its sides with the same letters as the previous hexagon, but primed (see Figure 4). Obviously, our trajectory τ in E is transported in E' by the cut and paste and we can code the trajectory with respect to the sides of the new hexagon. We will call this new cutting sequence $\bar{c}(\tau) \in \{A', B', C'\}^{\mathbb{Z}}$. The key remark is that we can write down $\bar{c}(\tau)$ if we know $\hat{c}(\tau)$. How? It is evident that if we have a trajectory in direction in Σ_0 , and a parallelogram with sides in directions 0 and $\frac{\pi}{6}$, knowing the cutting sequence with respect to the sides of the parallelogram gives automatically the intersections with the positive slope diagonal. Now, we can inscribe all the sides of E' in parallelograms made up of auxiliary edges (see Figure 4). This means that if we have the cutting sequence with respect to the auxiliary edges, we can "augment" the sequence with diagonals and erase the useless ones to obtain the cutting sequence with respect to the new

sides. It worth to draw the relative diagram \mathcal{D}'_0 , noticing that $A = A'$:



which records when, in a transition between two auxiliary sides (i.e. two sides of a parallelogram) we cross a primed side (i.e. a diagonal). This means that if we know the path which determines the sequence $\hat{c}(\tau)$, by reading the right letters ($A = A'$ and the labels of the arrows), we obtain $\bar{c}(\tau)$.

Fourth step: Up to changing the labels $A = A'$, $B \longleftrightarrow B'$ and $C \longleftrightarrow C'$ we have

$$\bar{c}(\tau) = c(\tau)'$$

In fact, $c(\tau)$ can be read on the diagram $\tilde{\mathcal{D}}_0$ by reading the label A and the labels of the arrows. Meanwhile, $\bar{c}(\tau)$ can be read on the diagram \mathcal{D}'_0 in the same way. This means that it is enough to compare the two diagrams $\tilde{\mathcal{D}}_0$ and \mathcal{D}'_0 , but it is easy to check that up to changing the letters as we said before, \mathcal{D}'_0 is obtained from $\tilde{\mathcal{D}}_0$ erasing from the arrow's labels exactly those letters which are not sandwiched.

Fifth step: Finally, by considering

$$\begin{aligned} \gamma: E' &\rightarrow E \\ B' &\mapsto B \\ C' &\mapsto C \\ \Upsilon_E^{-1}\tau &\mapsto \tau' = \gamma\Upsilon_E^{-1}\tau = \Upsilon_E^{-1}\gamma\tau = \Psi_\gamma\tau \end{aligned}$$

we exchange the labels as we needed in the previous step and we send the trajectory τ seen as $\Upsilon_E^{-1}\tau$ in E' after the cut and paste in the new trajectory τ' of the statement which will have cutting sequence with respect to $A = A'$, $B = \gamma B'$ and $C = \gamma C'$ the sequence $c(\tau') = \bar{c}(\tau) = c(\tau)'$ for the previous step and putting all together we have exactly as in the statement of the central proposition

$$c(\tau)' = c(\tau').$$

■

We wish to point out that the definition of γ as the orientation reversing element is useful in order to have in the end of the proof the same letters to substitute C' with C and B' with B . Obviously, nothing would change in the proof mixing the two labels, which are only symbols to identify edges, but using γ instead of σ allows us a simpler exposition.

1.3 Farey map

1.3.1 Definition

As in [Ser85a] for the square and in [SU11] for the $2n$ -gons, we want now to describe a way of producing a continued fraction expansion for the directions. Exactly in the same way and with the same proof as in [SU11] we will describe it as the itinerary of a map and use it to recover the direction of a trajectory given its cutting sequence.

We want to find out a way of acting with matrices on the space of directions \mathbb{RP}^1 . Each sector Σ_i corresponds to a sector $\tilde{\Sigma}_i \in \mathbb{RP}^1$ and each ν_i induces hence an action $\nu_i: \tilde{\Sigma}_i \rightarrow \tilde{\Sigma}_0$.

We now consider the angle coordinate in \mathbb{RP}^1 given by $\theta \in [0, \pi]$ and define the *Farey map* as the piecewise map defined on each Σ_i by the branch F_i given by the action of $\gamma\nu_i$.

Definition 1.19. The Farey map $F: \mathbb{RP}^1 \rightarrow \mathbb{RP}^1$ is defined in the angle coordinate θ , for $i = 0, \dots, 5$ by

$$F_i = \cot^{-1} \left(\frac{a \cot \theta + b}{c \cot \theta + d} \right), \quad \text{if } \theta \in \Sigma_i \text{ and } \begin{pmatrix} a & b \\ c & d \end{pmatrix} = \gamma\nu_i.$$

In Figure 5 is the graph of such a map in the coordinates.

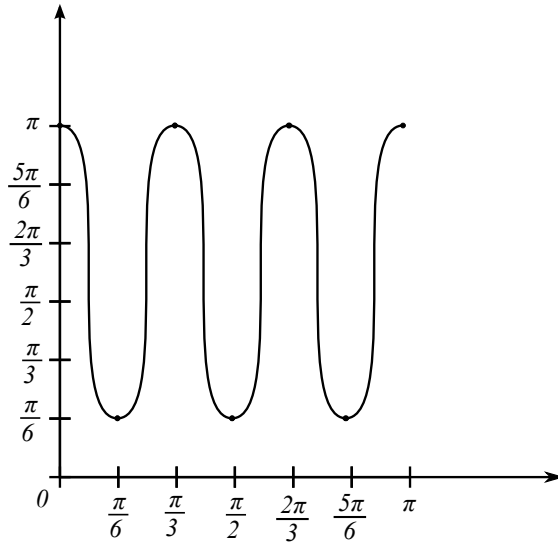


Figure 5: Graph of the Farey map

Remark 1.20. As the graph easily shows, it is a continuous map and since each branch is monotonic, they have an inverse map well defined. Moreover, the image of the Farey map is always contained in $[\frac{\pi}{6}, \pi]$.

Remark 1.21. The utility of the Farey map goes much further than we can explain here. Still, we can't miss to point out an important feature dealing with cutting sequences.

In fact, by the definition of the first branch F_0 , since ν_0 is the identity, we can find out something more about the trajectory τ' whose cutting sequence is the derived sequence of τ , as described in 1.18. In fact if τ is a trajectory in direction $\theta \in \Sigma_0$ as in the proposition, the new trajectory $\tau' = \Psi_\gamma \tau$ is in direction $F(\theta)$.

1.3.2 Hexagon Farey expansion

Starting from a $\theta \in [0, \pi]$ we can code its itinerary by applying repeatedly the right branch of F . In order to do that, we assign to the angle θ the sequence s_0, s_1, \dots such that $F^i(\theta) \in \Sigma_{s_i}$.

The previous remark, 1.20, shows us that such an itinerary is always such that $s_0 \in \{0, \dots, 5\}$, while $s_i \in \{1, \dots, 5\}$ for $i \geq 1$. We will call S^* such a subset of the set of sequences $\{0, \dots, 5\}^{\mathbb{N}}$.

As the itinerary of the Gauss map for the square gives the continued fraction expansion of the direction, in that case too the itinerary determines uniquely the direction θ at the beginning. In fact if we write

$$\Sigma[s_0; s_1, \dots, s_k] = F_{s_0}^{-1} F_{s_1}^{-1} \dots F_{s_k}^{-1}[0, \pi]$$

for the set of all direction whose itinerary starts with the segment s_0, s_1, \dots, s_k , with the same proof as in [SU11] for a given infinite itinerary $\{s_k\} \in S^*$ we can consider the intersection

$$\bigcap_{k \in \mathbb{N}} \Sigma[s_0, s_1, \dots, s_k]$$

and it turns out to be a unique number $\theta \in [0, \pi]$. we can then write $\theta = [s_0; s_1, \dots]$ and call the sequence $\{s_k\}$ the *hexagon Farey expansion of θ* .

1.3.3 Direction recognition

The problem posed and solved in this section is the following: is it possible to recover the direction of a non-periodic trajectory given its cutting sequence?

As we saw, we can associate to each direction an itinerary under the Farey map and conversely to each infinite sequence a unique direction it comes from. We will now relate such an itinerary with the cutting sequence of the trajectory.

Again, we won't write down the proofs, since they are exactly the same as those in the case of the octagon, which can be found in [SU11].

We will see shortly how useful is the hypothesis of non periodicity.

Let us consider a cutting sequence $w = c(\tau)$. We saw that a cutting sequence always represents a path in at least one of the diagrams \mathcal{D}_{d_0} . However, we want such d_0 to be well defined and hence we suppose that the cutting sequence $w = w_0$

is admissible in one unique diagram. We now consider the normal form of w as defined in 1.9 and set $w_1 = n(w)'$. Let us now suppose again that w_1 is admissible in only one diagram \mathcal{D}_{d_1} and define in the same way w_2 .

Applying the procedure recursively, we have defined the sequence of words $\{w_k\}_{k \in \mathbb{N}}$ as

$$\begin{cases} w_0 = w \\ w_{k+1} = n(w_k)' \end{cases}$$

and the sequence of admissible diagrams $\{d_k(w)\}_{k \in \mathbb{N}}$.

At each step we are assuming that the sequence is admissible in one unique diagram and that seems to be a quite restrictive hypothesis. Still, the condition can be proved to be quite simple and is actually exactly the condition we had at the beginning of the section: it can be proved that it is sufficient to ask that the trajectory of cutting sequence w is non-periodic.

This construction is what allows us to relate a cutting sequence with the Farey expansion of the direction of our trajectory, still supposed until now to be unknown. In fact, we have

Theorem 1.22. *If w is a non periodic cutting sequence with sequence of admissible diagrams $\{d_k(w)\}_{k \in \mathbb{N}}$, it is the coding of a trajectory in direction*

$$\theta = [d_0(w); d_1(w), d_2(w), \dots].$$

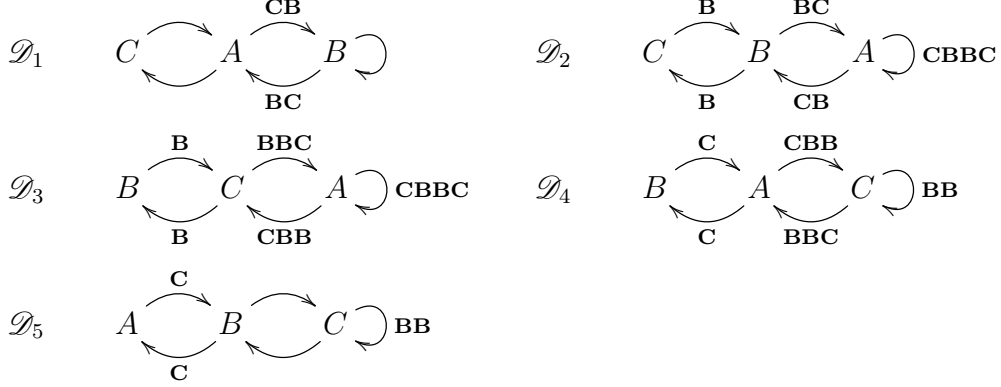
It remains to give a simple outline of what happens in the periodic case. The periodic case is based on the fact that periodic cutting sequences come exactly from periodic trajectories and they are related to the case of some directions for which we have an ambiguity in writing down the Farey expansion, either terminating with 1's or 5's.

1.4 Characterization

In this section we will introduce the full characterization of cutting sequences in the set of all sequences $\mathcal{A}^{\mathbb{Z}}$. Unfortunately, a straightforward characterization of the closure of cutting sequences as the set of infinitely derivable sequences (true in the case of the square) does not hold anymore. We will cite the additional condition in two different ways: the former following [SU11] and introducing the generation rules and the latter replacing them with the better known and more studied substitutions, which will be in a smaller number than the generation rules.

The generation is a combinatorial operation on words consisting of interpolating letters in a word and it wants to be an inverse operation to the derivation. We will denote this operator \mathbf{g}_i^j and applied to a word w admissible in diagram \mathcal{D}_i it will give us a word W admissible in diagram \mathcal{D}_j and whose derivative is $W' = w$.

The first generation operator \mathbf{g}_i^0 is obtained from the diagrams:



in the following way. Whenever we have a word admissible in diagram k we apply the operator \mathfrak{g}_k^0 by following the path represented by the word in the corresponding diagram and interpolating between letters the labels on each arrow. Explicitly, if in the original word we have the transition L_1L_2 and in the corresponding diagram the arrow that goes from L_1 to L_2 has the label $w_1w_2w_3w_4$ the new word will have the subword $L_1w_1w_2w_3w_4L_2$ instead.

It can be proved that for a w admissible in diagram \mathcal{D}_k , the new word $W = \mathfrak{g}_k^0w$ is admissible in diagram \mathcal{D}_0 and verify $W' = w$.

Definition 1.23. In a similar way we can define all the operators as

$$\mathfrak{g}_j^i w = \pi_i^{-1} \cdot \mathfrak{g}_j^0 w.$$

Again, applied to a word admissible in diagram \mathcal{D}_j it gives a word admissible in diagram \mathcal{D}_i whose derivative is the original word.

Then we have the following characterization:

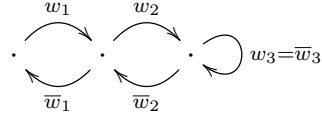
Proposition 1.24. *The sequence w is the cutting sequence of a trajectory in direction $\theta = [s_0; s_1, \dots]$ if and only if*

$$w \in \bigcap_{k \in \mathbb{N}} \mathfrak{g}_{s_1}^{s_0} \mathfrak{g}_{s_2}^{s_1} \dots \mathfrak{g}_{s_{k-1}}^{s_{k-2}} \mathfrak{g}_{s_k}^{s_{k-1}} u$$

where u is a word admissible in diagram \mathcal{D}_{s_k} .

This same characterization can be restated in terms of substitutions for both the hexagon and the octagonal case. It is useful because they are more used and especially because they allows us to give just five rules that can be applied in all cases instead of five different diagrams for each of the six admissible possibilities.

The idea is to notice that all diagrams have the same "shape" and to give a label to each arrow in the shape as follows:



where the conjugation means to read the label on the arrow from the right to the left which is coherent with the labels of augmented diagrams.

Each arrow of a diagram corresponds to a transition in the word represented by a path in such diagram and provided that from a word admissible in diagram \mathcal{D}_i we want a word admissible in diagram \mathcal{D}_j whose derivative is the original word, we will define the substitution σ_i on each arrow w_1, w_2, w_3 recording how the interpolated word of the diagram \mathcal{D}_i gives a path in the diagram \mathcal{D}_j . In other words, if an arrow w_k links two letters L_1 and L_2 and carries the label u_1u_2 we will record in $\sigma_i(w_k)$ the "name" of the arrows corresponding in the diagram \mathcal{D}_j to the transitions L_1u_1, u_1u_2, u_2L_2 . On the conjugated arrows they act as the same sequence of arrows, but read from the right to the left and with each element conjugated.

It can be seen that those substitutions are universal because applying permutations of the letters does not interfere and hence they can be obtained from the diagrams below.

A quick calculation show that they are

$$\begin{array}{l} \sigma_1 \left\{ \begin{array}{l} \sigma_1(w_1) = \bar{w}_1 \\ \sigma_1(w_2) = w_1w_2w_3 \\ \sigma_1(w_3) = w_3 \\ \sigma_1(\bar{w}_2) = \bar{w}_3\bar{w}_2\bar{w}_1 \\ \sigma_1(\bar{w}_1) = w_1 \end{array} \right. \quad \sigma_2 \left\{ \begin{array}{l} \sigma_2(w_1) = w_2w_3 \\ \sigma_2(w_2) = w_3\bar{w}_2\bar{w}_1 \\ \sigma_2(w_3) = w_1w_2w_3\bar{w}_2\bar{w}_1 \\ \sigma_2(\bar{w}_2) = w_1w_2w_3 \\ \sigma_2(\bar{w}_1) = w_3\bar{w}_2 \end{array} \right. \\ \\ \sigma_3 \left\{ \begin{array}{l} \sigma_3(w_1) = w_3\bar{w}_2 \\ \sigma_3(w_2) = w_2w_3\bar{w}_2\bar{w}_1 \\ \sigma_3(w_3) = w_1w_1w_3\bar{w}_2\bar{w}_1 \\ \sigma_3(\bar{w}_2) = w_1w_2w_3\bar{w}_2\bar{w}_1 \\ \sigma_3(\bar{w}_1) = w_2w_3 \end{array} \right. \quad \sigma_4 \left\{ \begin{array}{l} \sigma_4(w_1) = \bar{w}_2\bar{w}_1 \\ \sigma_4(w_2) = w_1w_2w_3\bar{w}_2 \\ \sigma_4(w_3) = w_2w_3\bar{w}_2 \\ \sigma_4(\bar{w}_2) = w_2w_3\bar{w}_2\bar{w}_1 \\ \sigma_4(\bar{w}_1) = w_1w_2 \end{array} \right. \\ \\ \sigma_5 \left\{ \begin{array}{l} \sigma_5(w_1) = w_1w_2 \\ \sigma_5(w_2) = \bar{w}_2 \\ \sigma_5(w_3) = w_2w_3\bar{w}_2 \\ \sigma_5(\bar{w}_2) = w_2 \\ \sigma_5(\bar{w}_1) = \bar{w}_2\bar{w}_1 \end{array} \right. \end{array}$$

The characterization becomes the following

Proposition 1.25. *The sequence w is the cutting sequence of a trajectory in direction $\theta = [s_0; s_1, \dots]$ if and only if there exists $w^{(k)}$ a sequence of arrows in $\{w_1, w_2, w_3, \bar{w}_2, \bar{w}_1\}$ such that*

$$w \in \bigcap_{k \in \mathbb{N}} \tau_{s_0} \sigma_{s_0} \sigma_{s_1} \dots \sigma_{s_k} w^{(k)}$$

where τ_{s_0} is the transformation of a sequence of arrows back in letters by following the path they form in \mathcal{D}_{s_0} .

1.5 Teichmüller disk

1.5.1 Marked translation surfaces and its actions

The derivation on cutting sequences is more than a mere combinatorial operator on it. As we will explain in this section, we can somehow identify the deformations of a given translation surface with the tangent bundle of the hyperbolic space (the Teichmüller disk), on which we will define a cutting sequence for a trajectory with respect to a tiling induced by a fundamental domain for the action of the Veech group on it. Then, we will relate the derivation previously defined and the new kind of cutting sequences.

First of all we need hence to explain what space are we going to work on. Given S translation surface, we can consider the space of *marked translation surfaces* as the space of translation surfaces correlated to S as follow:

Definition 1.26. If S is a translation surface and $f: S \rightarrow S'$ is an affine diffeomorphism from S to the translation surface S' such that the area of S is equal to the area of S' we say that S' is marked by S and identify the triples f, S, S' simply with $[f]$ with the convention that the function determines its domain and codomain.

Definition 1.27. We will also say that $[f] = f: S \rightarrow S'$ and $[g] = g: S \rightarrow S''$ are affinely equivalent if there exists a translation equivalence $[h] = h: S' \rightarrow S''$ such that $g = h \circ f$ and we will write $[f]_A$ for the affine equivalence class of the triple $[f]$.

Moreover, $[f]$ and $[g]$ are equivalent up to isometry if there exists an isometry $[h] = h: S' \rightarrow S''$ such that $g = h \circ f$ is an isometry and we will write $[f]_I$ for the isometry equivalence class of the triple $[f]$.

We will denote $\mathcal{M}_A(S)$ the set of translation surfaces marked by S up to affine equivalence and $\mathcal{M}_I(S)$ the set of translation surfaces marked by S up to isometry.

A simpler description of them can be made considering the following:

Proposition 1.28. *The set $\mathcal{M}_A(S)$ can be identified with $SL_{\pm}(2, \mathbb{R})$ and $\mathcal{M}_I(S)$ is isomorphic to $\mathbb{H} \simeq \mathbb{D}$.*

Here we are considering \mathbb{H} as the upper half plane $\mathbb{H} = \{z \in \mathbb{C} \mid \Im z > 0\}$ and $\mathbb{D} = \{z \in \mathbb{C} \mid |z| < 1\}$, identified to each other by $\phi: \mathbb{H} \rightarrow \mathbb{D}$ defined as $\phi(z) = \frac{z-i}{z+i}$.

We have two important actions on $\mathcal{M}_A(S)$ seen as the group of matrices. The first one we want to talk about is the left action of $SL_{\pm}(2, \mathbb{R})$ and in order to describe it, it is useful to give the explicit way of associating to a matrix a marked translation surfaces and the converse map, that is actually something we already talked about.

Indeed, we explained in 1.1.3 that if we have a matrix $\eta \in SL_{\pm}(2, \mathbb{R}) \subset GL(2, \mathbb{R})$ and a translation surface S , then we have a canonical map $\Phi_{\eta}: S \rightarrow \eta \cdot S$ such that $D\Phi_{\eta} = \eta$ and exactly that triple $[\Phi]$ is our marked translation surface in $\mathcal{M}_A(S)$. Conversely, to each map $f: S \rightarrow S'$ we associated the matrix Df .

Therefore the action of a new matrix $\nu \in SL_{\pm}(2, \mathbb{R})$ on a class of translation surfaces $[f]$ is the composition of the canonical map $\Psi_{\nu}: S' \rightarrow S''$ with f , obtaining $\Psi_{\nu} \circ f: S \rightarrow S''$. Using the identification in Proposition 1.28 and hence representing the set of marked translation surfaces as a space of matrices, the action is naturally the mere multiplication between matrices, applied on the left.

We have a second action on $\mathcal{M}_A(S)$ which is the action of $\text{Aff}(S)$. For an element $\Psi: S \rightarrow S$ in $\text{Aff}(S)$ it corresponds to the composition $f\Psi: S \rightarrow S'$. Again, using the identification in 1.28, that action is the multiplication on the right by the matrix $D\Psi$ representing the affine automorphism Ψ .

As one can easily see considering the actions as multiplications between matrices, the two actions naturally commute.

Let us now consider the action on $\mathcal{M}_A(S)$ of the particular subgroup g_t of $SL(2, \mathbb{R})$ defined by

$$g_t = \begin{pmatrix} e^{\frac{t}{2}} & 0 \\ 0 & e^{-\frac{t}{2}} \end{pmatrix}.$$

That particular action is called the Teichmüller flow and it can be proved that if we project $\mathcal{M}_A(S)$ in $\mathcal{M}_I(S)$ and use again the identification 1.28 it projects to the hyperbolic geodesic flow in the best way we can expect. In fact g_t -orbits in $\mathcal{M}_A(S)$ projects to unit speed parametrized geodesics in \mathbb{H} and we will call them *Teichmüller geodesics*.

We can explicitly give such an action writing down that the orbit of a marked translation surface $\Phi_{\nu}: S \rightarrow \nu \cdot S$ is the geodesic formed by the marked translation surfaces $[\Phi_{g_t\nu}]$ as $t \in \mathbb{R}$.

Moreover, let us now consider the map from $\mathcal{M}_A(S) \cong SL_{\pm}(2, \mathbb{R})$ to $T_1\mathbb{H}$ defined as follows: to a triple $\nu = [f]_A = \Phi_{\nu}: S \rightarrow \nu \circ S$ we associate the pair made of the point of \mathbb{H} given by the isometry class of the element $[f]_I = p_f$ and of the unit tangent vector in such point to the geodesic obtained by projecting the orbit of

$[f]_A$ under the g_t -action as explained before, i.e. the element $([f]_I = p_f, D\Phi_{g_t\nu} |_{t_0})$ where t_0 is the time of the flow such that $g_{t_0} = p_f$.

Such a map is a surjective 4 to 1 map. For simplicity, we will firstly identify the two copies of the upper and lower half plane \mathbb{H}^+ and \mathbb{H}^- and then make the quotient with the Kernel of the new map $\{\pm \text{Id}\}$ and hence consider the marked translation surfaces as $PSL(2, R)$ obtaining a 1 to 1 map in $T^1\mathbb{H}$ and hence an identification of the two spaces.

We now return to our case of the surface obtained from the hexagon S_E and consider the marked translation surfaces affinely equivalent to S_E , identified with $T^1\mathbb{D}$ and by the correspondence with $PSL(2, \mathbb{R})$. The centre of the disk will be identified with the identity matrix and hence with the triple $\text{Id}: S_E \rightarrow S_E$. As we saw before, we have the action of the Veech group on it and it turns out that we can explicitly give a fundamental domain for such an action.

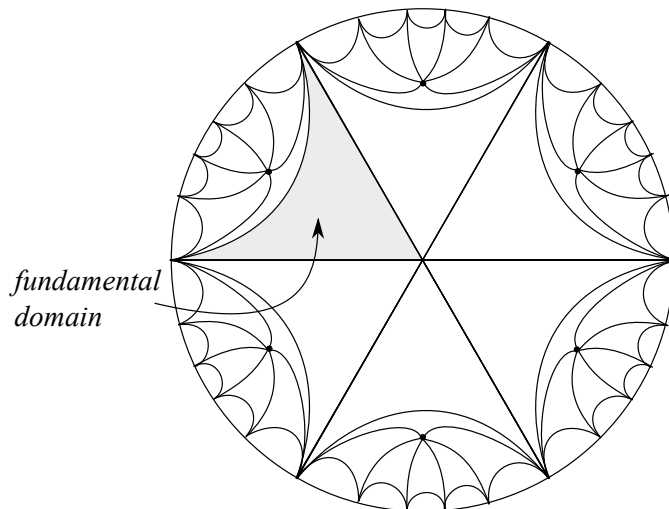


Figure 6: Fundamental domain tessellation

Let us consider the hyperbolic triangle formed by the horizontal line between the centre of the disk and the extreme left point of the boundary, the line between the boundary and the centre forming angle $\frac{\pi}{3}$ with the previous one and the third geodesic joining the two boundary points as in Figure 6. We will call it \mathcal{F} and we affirm that it is a fundamental domain for the action of the Veech group. Indeed, the three generators of such group α, β, γ are hyperbolic reflections with respect to the three sides of \mathcal{F} and hence the Veech group is the triangular group $\Delta(3, \infty, \infty)$.

In fact if we apply on the left (being a left action) α to an element of \mathbb{H} seen as a pair and then send it in \mathbb{D} with the map describe before, we have that point reflected in the disk with respect to the horizontal side. In the same way, applying β means reflecting with respect to the geodesic passing for the centre of the disk and forming angle $\frac{\pi}{3}$ with the horizontal left oriented line and γ is the reflection with respect to the third side.

The images under the Veech group of the fundamental domain give a tiling of the Teichmüller disk.

1.5.2 Teichmüller geodesics and hexagonal tiling

We will now introduce a special type of geodesics in the Teichmüller disk and a second tiling on it and explain how we can code the flow of such a geodesic with respect to such a tiling. In the next paragraph, we will see how that is related with the coding of trajectories in the surface S_E and particularly with the derivation.

Let us fix a direction θ , and think about it as the direction of a trajectory τ in S_E . We can hence consider the subgroup conjugate to the geodesic flow introduced before

$$g_t^\theta = \rho_{\frac{\pi}{2}-\theta}^{-1} \circ g_t \circ \rho_{\frac{\pi}{2}-\theta}.$$

Geometrically, as t increase, since g_t expands the horizontal direction and contracts the vertical one, and the conjugation with the counterclockwise rotation of angle $\frac{\pi}{2} - \theta$ sends the direction θ in a vertical position and sends it back, such a subgroup contracts the direction θ and expands the orthogonal direction.

Let us now call *Teichmüller geodesic ray*

$$\tilde{r}_\theta = \{g_t^\theta \cdot S_E\}_{t \geq 0}$$

which is a geodesic ray in $T_1\mathbb{D}$ and denote r_θ its projection on \mathbb{D} . Naturally, r_θ is a geodesic ray in \mathbb{D} , starting in the centre of the disk and converging to a point of the boundary. The mere calculation of the matrix

$$g_t^\theta = \begin{pmatrix} e^t \sin^2 \theta + e^{-t} \cos^2 \theta & -e^t \sin \theta \cos \theta + e^{-t} \sin \theta \cos \theta \\ -e^t \sin \theta \cos \theta e^{-t} \sin \theta \cos \theta & e^t \cos^2 \theta + e^{-t} \sin^2 \theta \end{pmatrix}$$

and its action on i (which means imposing the geodesic to pass for i), shows that the limit as $t \rightarrow \infty$ is the boundary point $-\tan \theta \in \partial\mathbb{H}$ which is sent by the identification of \mathbb{H} and \mathbb{D} in the boundary point $e^{i(\pi-2\theta)}$ since it is

$$\begin{aligned} -(\cos^2 \theta - \sin^2 \theta) + 2i \cos \theta \sin \theta &= -\cos 2\theta + i \sin 2\theta = \\ &= \cos(\pi - 2\theta) + i \sin(\pi - 2\theta) = \\ &= e^{i(\pi-2\theta)}. \end{aligned}$$

This makes it easier to understand how the angle θ parametrizes the boundary and equivalently the geodesic rays coming out from the centre of the disk: the ray r_0 is the one corresponding to the horizontal line oriented on the left and the generic ray r_θ is the one which form a clockwise angle of 2θ with the ray r_0 . This means that as θ run along the interval that we always considered up to apply a π -rotation, it parametrize all the boundary of the disk.

If we now return to consider the image of the fundamental domain \mathcal{F} under the Veech group, we can naturally act with the six elements ν_i explained in the first section. We call E_0 the side connecting the two boundary points and we can define E_1, \dots, E_5 as $E_i = E_0\nu_i$ meaning the right action of ν_i on each point composing the side. We hence have an hyperbolic hexagon \mathcal{E} limited by the sides E_0, \dots, E_5 and by acting on it with the Veech group we obtain a new tessellation of the disk \mathbb{D} the *ideal hexagon tessellation*, obtained by the previous one deleting the tile sides joining an image of the centre of the disk, i.e. consider as one unique tile all six triangles sharing one common vertex as in Figure 7.

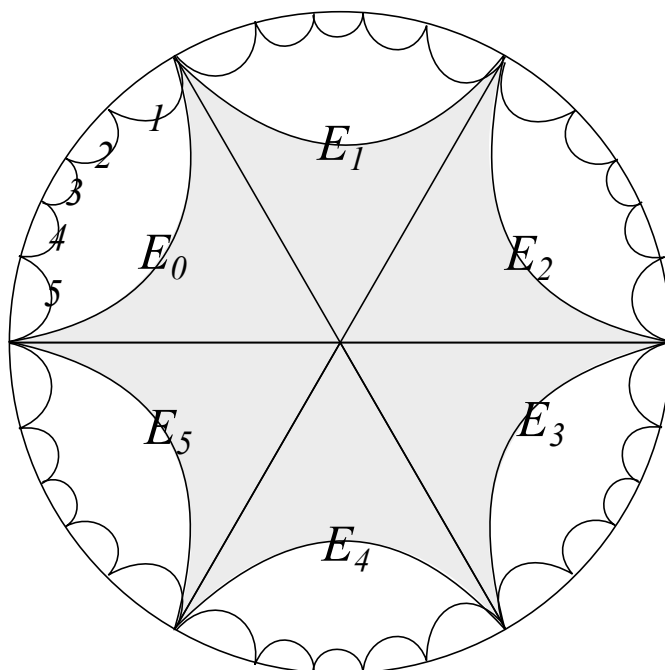


Figure 7: Ideal hexagons tessellation

Remark 1.29. For the parametrization of the boundary with the angle as described before, we have that a Teichmüller geodesic ray r_θ crosses the side $E_i = E_0\nu_i$ if and only if $\theta \in \Sigma_i = \nu_i^{-1}\Sigma_0$.

Such an ideal hexagon tessellation allows us to construct a tree related to it. It will be useful to explain the propositions in the following section.

The set of vertices of such a tree is the set of centres of the ideal hexagons, i.e. the images under the action of the Veech group of the centre of the disk. The edges will be geodesic segments connecting two centres if and only if the two hexagons share a common side. Naturally, we can consider such a tree not embedded in the hyperbolic disk and have segments joining the vertexes. We will have hence a regular tree \mathcal{T} with six edges coming out of each vertex.

To each Teichmüller geodesic ray we can associate a path in the tree \mathcal{T} that we will call *combinatorial geodesic* P_θ approximating r_θ . If r_θ does not terminate in a vertex of the tessellation (and it can be proved that it corresponds to the case of periodic trajectories that we didn't consider since the beginning), it intersects an infinite number of sides of ideal hexagons. We associate to it a path starting from the centre of the disk and crossing all the couple of vertexes which are the two centres of the two hexagons which share the side crossed by r_θ .

1.5.3 Teichmüller cutting sequences

By giving a label to each segment of the tessellation with ideal hexagon, we can assign to each Teichmüller geodesic a *Teichmüller cutting sequence* by coding the intersections of the geodesic with the labels assigned to each side. It turns out that there is an intimate connection between the derivation that we used in the first part of the work on cutting sequences on trajectories in the surface S_E and the Teichmüller cutting sequences.

This is a similar procedure to the one described by Series in [Ser85b].

In order to label the sides of the tiling, we introduce the subgroup of the Veech group $V_{\mathcal{E}}$. It is the subgroup generated by the hyperbolic reflections with respect to the sides of \mathcal{E} , that can be obtained by conjugating the reflection with respect to the side E_0 (which is our matrix γ) by the matrices ν_i introduced at the beginning of the work. $V_{\mathcal{E}}$ is hence the subgroup generated by $\gamma_i = \nu_i^{-1}\gamma\nu_i$ for $i = 1, \dots, 5$.

The hexagon \mathcal{E} is a strict fundamental domain for such a group and this allows us to label each side of the tiling in the following way: given a side, there is an element of $V_{\mathcal{E}}$ that sends it back in a side E_i of \mathcal{E} and we label such a side of the tiling with the number $i \in \{0, \dots, 5\}$.

We can also use it to give a labelling on the tree \mathcal{T} by labelling each edge with the number of the side of the tiling transversal to it.

Remark 1.30. For each side shared by two ideal hexagons, if it is labeled with i , it will exist $n \in \mathbb{N}$ and a sequence $\{s_k\}_{k=0, \dots, n} \in \{0, \dots, 5\}$ such that one ideal hexagon is $\mathcal{E}\gamma_{s_n}\gamma_{s_{n-1}} \dots \gamma_{s_1}\gamma_{s_0}$ and the other one is $\mathcal{E}\gamma_i\gamma_{s_n}\gamma_{s_{n-1}} \dots \gamma_{s_1}\gamma_{s_0}$.

Given a geodesic in the Teichmüller disk, we define the *Teichmüller cutting sequence* associated to it as the sequence of labels of sides of the ideal hexagon tessellation crossed by the geodesic. In particular, we can do that for a Teichmüller geodesic ray r_θ and associate to it $c(r_\theta) \in \{0, \dots, 5\}^{\mathbb{N}}$. It represents also the labels of the edges forming the path p_θ in \mathcal{T} correspondent to the ray r_θ .

Remark 1.31. It is evident that since a cutting sequence never returns back, in a Teichmüller cutting sequence the same label never occurs twice in a row. Moreover, it can be seen that it is the only restriction that one needs on an element of $\{0, \dots, 5\}^{\mathbb{N}}$ for being a Teichmüller cutting sequence.

In exactly the same way as in [SU10] we can prove the relation between the Teichmüller cutting sequences of a ray r_θ and the cutting sequence of a trajectory in direction θ , as in the following proposition, which gives a geometrical interpretation of the derivation on a cutting sequence.

Let us consider w cutting sequence of a trajectory τ in direction θ , its k -derived sequence $w^{(k)}$ and the corresponding Teichmüller geodesic ray r_θ with Teichmüller cutting sequence $c(r_\theta)$.

We define for each $k \geq 1$ the element of the Veech group $\gamma^{(k)}$ as the composition of $\gamma_{s_{k-1}} \gamma_{s_{k-2}} \dots \gamma_{s_0}$ where s_0, \dots, s_{k-1} are the first entries of the Teichmüller cutting sequence $c(r_\theta)$. Such an element sends the k -th ideal hexagon crossed by r_θ back in \mathcal{E} by Remark 1.30. As we did before for the elements of the Veech group, we have a correspondent affine automorphism $\Psi_{\gamma^{(k)}}: S_E \rightarrow S_E$ whose derivative is $\gamma^{(k)}$ as the composition of the canonical map $\Phi_{\gamma^{(k)}}: S_E \rightarrow \gamma^{(k)} \cdot S_E$ and the cut and paste map $\Upsilon^{(k)}: \gamma^{(k)} \cdot S_E \rightarrow S_E$. On the original hexagon this automorphism consists in applying an affine deformation and then cutting and pasting it back in the original hexagon. Such deformation stretches the direction θ in the hexagon.

Proposition 1.32. *The k -th derived sequence $w^{(k)}$ of a cutting sequence w of a trajectory τ in direction θ in S_E is the cutting sequence of the same trajectory with respect to the sides of $\Psi_{\gamma^{(k)}}E$ with the labelling induced by $\Psi_{\gamma^{(k)}}$.*

Proof. Saying that $w^{(k)}$ is the cutting sequence of τ with respect to $\Psi_{\gamma^{(k)}}E$ is equivalent to say that $w^{(k)}$ is the cutting sequence of $\Psi_{\gamma^{(k)}}^{-1}\tau$ with respect to E .

We prove it by induction. For the case $k = 0$ it is just $w = c(\tau)$.

For $k > 0$ let's set

$$\begin{cases} \tau_0 = \tau \\ \tau^{(k)} = \Psi_{\gamma^{(k)}}^{-1}\tau = \Psi_{\gamma_{s_{k-1}}} \dots \Psi_{\gamma_{s_0}}\tau. \end{cases}$$

Our aim becomes to show that $w^{(k)}$ is the cutting sequence of $\tau^{(k)}$ for each $k > 0$.

We now assume as inductive hypothesis that $w^{(k)}$ is the cutting sequence of $\tau^{(k)}$.

The trajectory $\tau^{(k)}$ has direction in Σ_{s_k} for Remark 1.29. This means that $\nu_{s_k}\tau^{(k)}$ has direction in Σ_0 and hence its cutting sequence is $\pi_{s_k} \cdot w^{(k)}$ for 1.1. Let us now derive once more in order to obtain $w^{(k+1)}$. We have

$$(\pi_{s_k} \cdot w^{(k)})' = c(\Psi_\gamma \nu_{s_k} \tau^{(k)})$$

for Proposition 1.18. Now we act with $\nu_{s_k}^{-1}$ on the trajectory $\Psi_\gamma \nu_{s_k} \tau^{(k)}$ so that it becomes exactly $\tau^{(k+1)}$ and we have

$$\begin{aligned} c(\tau^{(k+1)}) &= c(\Psi_{\gamma_{s_k}} \tau) = c(\nu_{s_k}^{-1} \Psi_\gamma \nu_{s_k} \tau^{(k)}) = \\ &= \pi_{s_k}^{-1} \cdot (\pi_{s_k} \cdot w^{(k)})' = \pi_{s_k}^{-1} \cdot \pi_{s_k} \cdot (w^{(k)})' = w^{(k+1)} \end{aligned}$$

using again 1.1 and then 1.8 and hence the thesis. ■

2 Hexagon vs square

In this section we will try to investigate two aspects of differences and similarities between hexagon and square.

In the first part we point out that the derivation in the Series method for the square is slightly different from the one used for the hexagon here and for the octagon in [SU11] and we show how to adapt the second one to the case of the square too.

In the second part we will show where is the hexagon located in the space of flat tori and we will construct a dictionary between the hexagon and its representative as a parallelogram.

2.1 Derivations in the square

At a first reading [Ser85a] and [SU11] seem to have three different definitions of the operation of derivations

1. In the case of the square a cutting sequence consists in blocks of length n_0 or $n_0 + 1$ of the same letter separated from one occurrence of the other one. Series's derivation in [Ser85a] consists of erasing n_0 letters from each block before interchanging the roles of the two letters.
2. In [SU11], the derivation used in the case of the square consists in erasing one letter from each block until possible before interchanging the roles of the two letters.
3. The method used here for the hexagon (as well as in [SU11] and [Dav13] for regular octagons and double regular pentagons) is to keep the sandwiched letters and drop the others.

2.1.1 Series derivation

The difference between 1. and 2. can be easily explained. In fact, the Series derivation is nothing but an acceleration of the one described by Smillie and Ulcigrai. This difference is related to the fact that the n -th branch of the Gauss map used by Series is just $G_n = F_1 \circ F_0^{n-1}$ on the interval $[\frac{1}{n+1}, \frac{1}{n}]$, as we verified by induction.

2.1.2 Where sandwich derivation fails

On the other hand, the difference between the Series derivation and the sandwich derivation remains a real difference. Consider a square Q with opposite sides glued obtaining the surface S_Q and try to follow the same procedure as for the hexagon. Since we have one more symmetry we can immediately reduce to the case of a

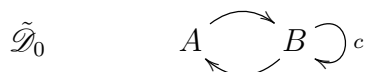
trajectory τ in direction $\theta \in [0, \frac{\pi}{2}]$ and by applying ν_1 , reflection with respect to the bisectrix of the first quadrant and the permutation $\pi_1 = (AB)$ we can always send a direction in $[0, \frac{\pi}{4}]$. The cylinder decomposition of the square in a unique cylinder given by the square itself gives us the Veech element used by Series:

$$\sigma = \begin{pmatrix} 1 & 1 \\ 0 & 1 \end{pmatrix}.$$

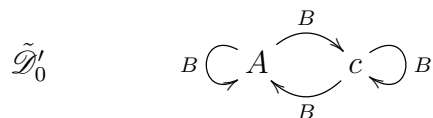
Remark 2.1. We notice that applying the shear σ or its orientation-reversing counterpart $\gamma = \begin{pmatrix} -1 & 1 \\ 0 & 1 \end{pmatrix}$ in this case does not change anything because the reflection with respect to the vertical axis does not change labels.

Unfortunately, if we try to characterize cutting sequences as before we need to show that cutting sequences are infinitely derivable, but if we try to reproduce the proof of Proposition 1.18 we do not get to the same conclusion.

In the first step we construct the augmented sequences $\tilde{c}(\tau) \in \{A, B, c\}^{\mathbb{Z}}$ by recording on the diagram $\tilde{\mathcal{D}}_0$ the intersection with the diagonal c :



In the second step we interchange the role of B and c obtaining $\hat{c}(\tau) \in \{A, c\}^{\mathbb{Z}}$ and the diagram



In the third step we apply the cut and paste map Υ_Q that act sending the polygon deformed by the Veech shear back in the original polygon, but we find out that since $A' = A$ and $B' = c$ the cutting sequence $\bar{c}(\tau)$ of the trajectory with respect to the sides A', B' of the new square $Q' = \sigma Q$ is exactly the previous one $\hat{c}(\tau)$. As we see in Figure 8, this is because the new side coincide with the diagonal instead of being inscribed in a parallelogram formed by previous sides and diagonals, which determined uniquely which of the new sides are crossed.

2.1.3 How sandwich derivation can work

At this point we tried to understand if there is a way to adapt the procedure used for the hexagon to make it work in the case of the square too. It turns out that it is possible to make it work just using a slightly different matrix.

In fact in the cases of $2n$ -gons for $n \geq 3$ we always used as Veech shears the matrices

$$\begin{pmatrix} 1 & 2 \cot\left(\frac{\pi}{2n}\right) \\ 0 & 1 \end{pmatrix}$$

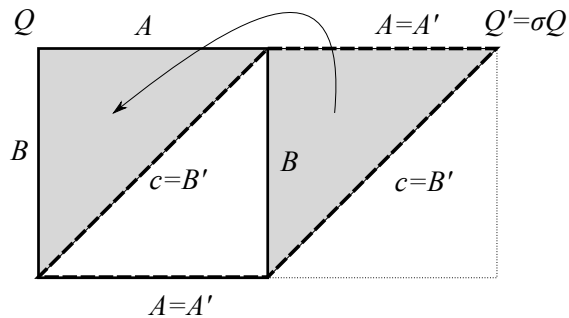


Figure 8: Action of the Veech element and of the cut and paste map on the square

which in this case is not the shear σ given by the cylinder decomposition but the composition

$$\sigma' = \sigma^2 = \begin{pmatrix} 1 & 2 \\ 0 & 1 \end{pmatrix}.$$

Using this matrix instead of the previous one is the same than considering the square rotated by $\frac{\pi}{4}$, obtaining a diamond-shape and looking for an horizontal cylinder decomposition. The decomposition showed in Figure 9 gives us a cylinder of modulus exactly 2.

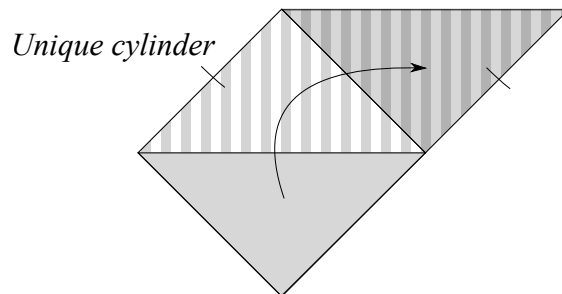


Figure 9: Horizontal cylinder decomposition for the rotated square

Using this matrix we can continue to reproduce the proof of Proposition 1.18 and we have first and second step as before.

For the third step, after applying the cut and paste Υ'_Q showed in Figure 10 the new side B' is in this case the diagonal of a parallelogram with sides A and the diagonal c as we wanted.

This means that we can construct the diagram recording the crossing of the sides of the new square as

$$\mathcal{D}'_0 \quad B' \circlearrowleft A \circlearrowright c \circlearrowleft B'$$

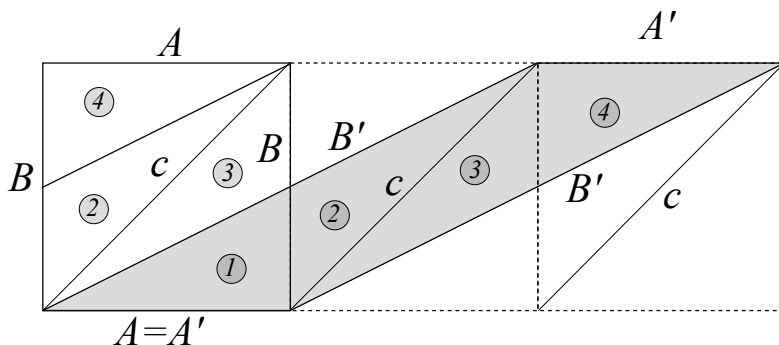


Figure 10: Veech shear and cut and paste with the new matrix

and by looking at diagrams \mathcal{D}'_0 and $\tilde{\mathcal{D}}'_0$ as in the original proof we notice again that the sandwiched letters are the one kept.

We can conclude that sandwich derivation gives us a different way of characterizing the cutting sequences in a square. We already knew that cutting sequences in the square are infinitely derivable in the Series sense and we have now proved that cutting sequences in the square are infinitely derivable also in the sense of sandwich derivation.

Exactly as before, we can construct a Farey map different from the previous one.

In the Teichmüller disk of the deformations of the square, using the new matrix one can repeat exactly the same proofs as in the case of the hexagon. The correspondent matrix $\gamma' = \begin{pmatrix} -1 & 2 \\ 0 & 1 \end{pmatrix}$ is the hyperbolic reflection with respect to the geodesic passing through 0 and 1 and hence we have the two tessellations by hyperbolic triangles and by hyperbolic squares exactly as before, by considering the two matrices

$$\alpha = \begin{pmatrix} 1 & 0 \\ 0 & -1 \end{pmatrix}, \quad \beta = \begin{pmatrix} 0 & 1 \\ 1 & 0 \end{pmatrix}$$

which are, as in the case of the hexagon, the reflection with respect to the horizontal axis and the matrix ν_1 .

Proposition 1.32 can be also stated and proved in the same way for the case of the square.

2.2 Hexagon as a flat torus

2.2.1 Space of flat tori

The space of flat tori is the space of lattices in the plane. We identify a lattice with its two-dimensional basis $\mathbb{Z}v_1 + \mathbb{Z}v_2$. Conventionally, up to change v_1 and

v_2 we can consider v_1 to have smaller length. Up to rotating and scaling, we can suppose v_1 to be coincident with the first vector of the classic basis in the plane e_1 and the basis to be positively oriented, so that v_2 is in the upper half plane that we identify with \mathbb{H} . But we can restrict the domain even more, because acting with an element of $SL(2, \mathbb{Z})$ we obtain the same lattice because we just change the length of a integer and hence we can quotient the upper half plane by this group. This means the following:

Proposition 2.2. *The space of flat tori, i.e. the space of lattices is*

$$\mathbb{H}/SL(2, \mathbb{Z}),$$

where $SL(2, \mathbb{Z})$ is considered acting on the right by Möbius transformations.

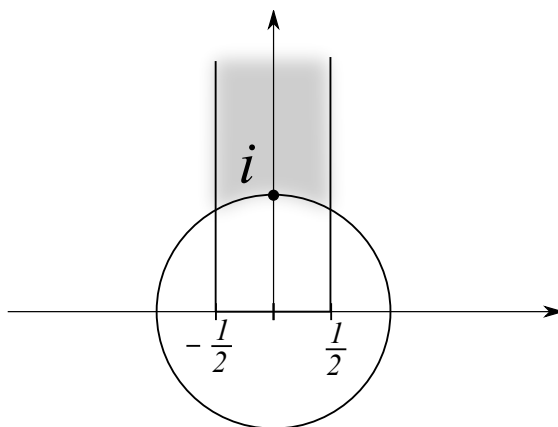


Figure 11: The space of lattices

It is well known that a fundamental domain for the $SL(2, \mathbb{Z})$ action is the infinite region limited by the vertical lines through $\frac{1}{2}$ and $-\frac{1}{2}$ and the upper semicircle of the unit circle.

It is also known that the hexagon is represented by the intersection point of the semicircle with the imaginary axis.

Naturally, this implies that we cannot find a cut and paste from the hexagon to the square, even if they both represent flat tori. This means also that with a cut and paste map we can send the hexagon in a parallelogram with the bottom left angle of $\frac{\pi}{3}$. In fact the modulus of such a parallelogram seen as a cylinder is the same of the modulus of the unique cylinder of the horizontal cylinder decomposition of the hexagon and it is clear that the modulus of the parallelogram determines its position in the space of flat tori.

2.2.2 Dictionary

Let us now add to the figure of an hexagon the diagonals e and f starting from the bottom left angle and such that the first one is vertical and the second one is

in direction $\frac{\pi}{6}$ as in Figure 12. We can cut the hexagon along these diagonals and paste the two smaller pieces on the sides labelled B and A of the hexagon, so that the two sides labelled C are glued together.

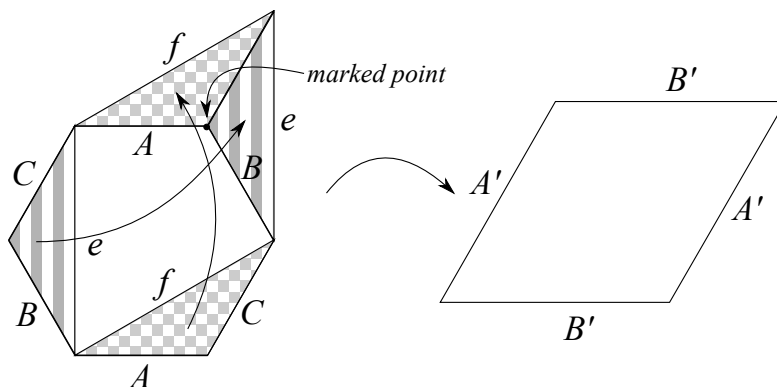
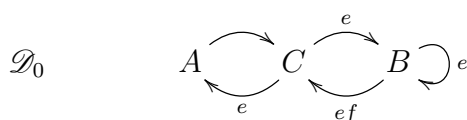


Figure 12: Cut and paste from the hexagon to the parallelogram

The cut and paste map we just described is showed in Figure 12. Up to rotating the figure we have obtained the requested parallelogram, equivalent to the hexagon and representing it in the fundamental domain of $SL(2, \mathbb{Z})$, which is the space of flat tori, as we explained before.

Let us consider a trajectory in a direction belonging to Σ_0 in the hexagon. It naturally is also a trajectory in such a parallelogram P . Suppose we have the cutting sequence of such a trajectory with respect to the sides of E . In order to find out the cutting sequence with respect to the sides of P we first record the passage for the diagonals e and f in the transition diagram \mathcal{D}_0 .

The diagram becomes hence:



This allows us to construct an *augmented sequence* recording both the passages for the sides of the hexagon and of the parallelogram. To obtain the cutting sequence with respect to P we just need to eliminate the record of the crossing of A , B and C by dropping those letters from the cutting sequence and then substitute e with A' and f with B' .

The new sequence in $\{A', B'\}^{\mathbb{Z}}$ is the cutting sequence of the same trajectory with respect to the sides of the parallelogram P .

Remark 2.3. We can consider just the case of a trajectory in direction in Σ_0 because if the trajectory is in a direction in Σ_i we can apply ν_i and repeat the procedure. The unique difference is that we have to consider different diagonals e and f such that after applying ν_i they are sent in the diagonals considered in the case of trajectories in Σ_0 .

2.2.3 Relations

Unfortunately, no matter which derivation procedure do we use, the derivation and the dictionary do not commute. A simple counter-example is the trajectory in horizontal direction passing for the midpoint of the sides B and C . Its cutting sequence is the periodic word obtained repeating the sub-word BC . Its sandwich-derived sequence is the same word and by applying the dictionary the same trajectory has cutting sequence with respect to P given by the periodic word obtained repeating $A'B'B'$ whose derivative (both the Series one and the sandwich one) is not the same sequence.

Another explanation for this is because although the hexagon and the parallelogram are the same flat tori, by applying the cut and paste map we are losing the information of the second marked point that we have in S_E , since after the cut and paste it becomes a point in the interior of the parallelogram, which gives a torus with just one marked point corresponding to the four vertices.

Moreover, if we consider the tessellation of the Teichmüller disk in the case of the hexagon and the one of the square (either the construction given by Series in [Ser85b] or the one presented in the previous section) the two seem not to be in any way comparable. In fact, one sees the disk divided in six sectors and the second in four sectors, crossing the boundary in different points.

3 Cutting sequences for a Bouw-Möller surface

The last case we will try to analyse in this work is the one of a Bouw-Möller surface.

They were first discovered and described in an algebraic way by Irene Bouw and Martin Möller in [BM10] as the surfaces having Veech group isomorphic to the triangular group $\Delta(m, n, \infty)$. Hence it is still a Veech surface as the previous cases of squares, regular $2n$ -gons and regular double odd-gons, which has also triangular groups as Veech groups.

Later, Pat Hooper in [Hoo12] gave a flat description of those surfaces as surfaces obtained by gluing together a finite number of semi-regular polygons.

Some new results about cutting sequences in Bouw-Möller surfaces are obtained by Diana Davis, who is working on it, but her approach is deeply different from ours, since she does not use at all the second representation of Bouw-Möller surfaces described by Hooper, which has a key role in our results. In fact, it appears in our main result presented in this work, which is Theorem 3.6 and state that the derived sequence of a cutting sequence of a trajectory in the Bouw-Möller surface $\mathcal{M}(3, 4)$ is still a cutting sequence.

3.1 Two representations of the surface

As described in [Hoo12] to each Bouw-Möller surface we can associate a grid graph and viceversa. Since we have two different ways of obtaining a decomposition in semi-regular polygons from a graph, this means that each graph has two different representations in semi-regular polygons, considering $\mathcal{G}(m, n)$ or $\mathcal{G}(n, m)$. Since we always obtain two-dimensional graphs, each Bouw-Möller surface is identified by two parameters m and n which will be the number of rows plus one and the number of columns plus one. The corresponding surface will be denoted $\mathcal{M}(m, n)$. Here we will call $\mathcal{M}(m, n)$ and $\mathcal{M}(n, m)$ the two representations of $\mathcal{M}(m, n)$, because associated to the same graph and affinely equivalent.

Let us start from the representation of the surface S as a regular octagon with two squares glued to it as in Figure 13, where all sides have unit length.

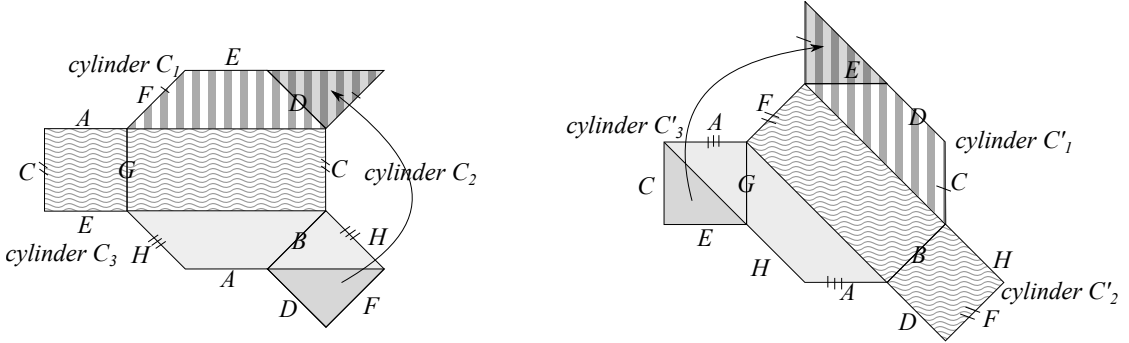


Figure 13: First representation of $\mathcal{M}(3, 4)$ and cylinder decompositions.

To construct the related grid graph we consider the cylinder decompositions in Figure 13, the horizontal one and the one in direction $\frac{3\pi}{4}$. The set of vertices will be a bipartite one, $V = V_b \cup V_w$ and we will denote V_b and V_w in figures by black dots and white dots. Each vertex represents a cylinder and vertices in V_b are in 1 to 1 correspondence with horizontal cylinders, while black dots are in 1 to 1 correspondence with cylinders in direction $\frac{3\pi}{4}$.

An edge between two vertices v_i and v'_j represents the basic parallelogram which is the intersection of the two corresponding cylinders $C_i \cap C'_j$.

On each vertex we establish an order on the edges coming out of that vertex by adding circular arrows turning clockwise on the odd columns of the graph and counter-clockwise on the even ones and register which basic parallelograms are glued together.

In this way we can construct the grid graph that turns out to be as in Figure 14.

As the number of rows and columns are two and three this explains why we call such a surface $\mathcal{M}(3, 4)$.

Conversely, we can find out the two representations by "decomposing" the

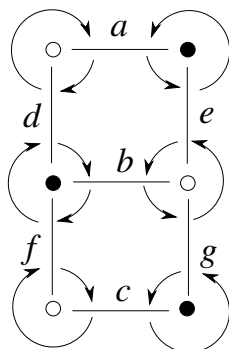
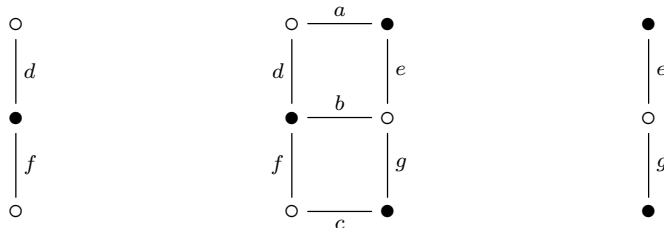


Figure 14: Grid graph of $\mathcal{M}(3,4)$.

diagram in smaller pieces, each of which corresponds to one polygon (regular or semi-regular) of the representation.

By decomposing it in vertical, in fact, we obtain the three pieces:



Now each edge, denoted by a letter, corresponds to a basic parallelogram (of side length still to be determined) in our decomposition but in general we do not know the directions of the cylinder decompositions used and hence the slope of the parallelograms. Up to shear the representation obtained, we hence now consider them as basic rectangles. The ones repeated twice correspond each time to half a rectangle (i.e. a triangle) in each piece of the decomposition.

The arrows between edges that we have on the graph show us how the basic rectangles are glued. Since vertices in V_w represent horizontal cylinders, an arrow rotating around a vertex in V_w between two edges means that the right side of the basic rectangle corresponding to one edge is glued to the left side of the basic rectangle corresponding to the other edge. Conversely, since vertices in V_b represent vertical cylinders, arrows around vertices in V_b correspond to basic rectangles glued through top and bottom sides.

For example let us compare the second piece of the graph and the second polygon in Figure 15 which shows the first representation. In the graph, there is an arrow connecting edges a and d around a white vertex and hence a and d are glued on the right and left side respectively. The arrow between edges d and b is around a black vertex and hence they are glued through the top and bottom sides. Moreover, the basic rectangle corresponding to b is glued to d and f by the top

and bottom sides since the arrows connecting the edge b and the edges d and f are around a black vertex. And it is glued to e and g by the right and left sides because the arrows connecting them are around a white vertex.

This allows us to give the first decomposition R_1^\perp (see Figure 15) that turns out to be exactly as before, two quadrilaterals and a octagon, but sheared so that the two cylinder decomposition described before are orthogonal. To have back the regular decomposition we have to apply the shear sending the orthogonal lines back in direction $\frac{3\pi}{4}$. We will call such sheared representation R_1 and the one with orthogonal cylinder decompositions R_1^\perp .

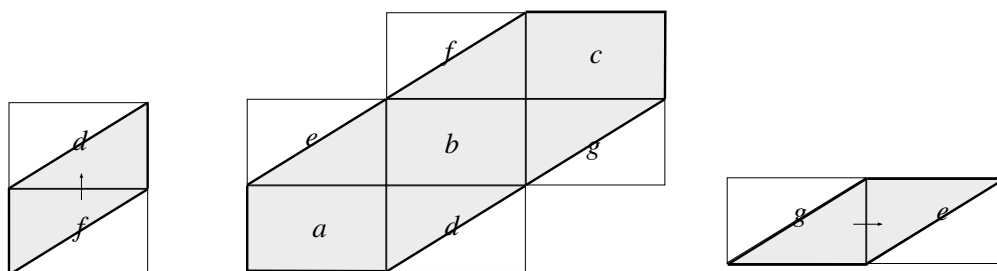
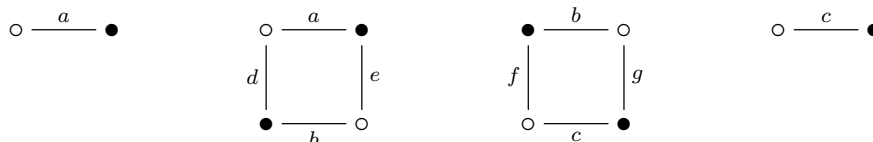


Figure 15: The representation R_1^\perp .

By decomposing the grid graph in horizontal, we obtain the second representation. We get the decomposition



and repeating the same procedure described above we have the decomposition in Figure 16 that we will denote R_2^\perp . It can be sheared back in two triangles and two semi-regular hexagons. We will call the second representation R_2 and is represented in Figure 17 together with the two cylinder decompositions which becomes orthogonal in the representation R_2^\perp .

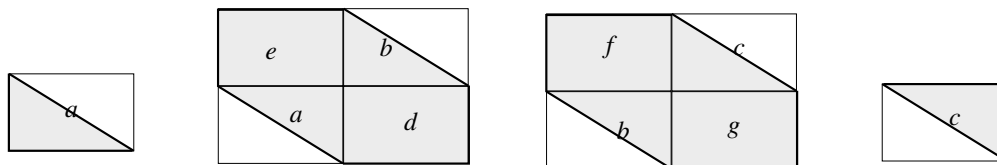


Figure 16: The representation of R_2^\perp .

In [Hoo12], Hooper describes how to determine the lengths of the sides of the basic rectangles and hence the sides of the polygons from the graph. The

first decomposition is made of regular polygons, a kind of particular case of semi-regular polygons where one of the sizes of sides is zero. So all sides has same length that we fix to be 1. In the case of the hexagon, we find out that the two triangles are equilateral and with sides of the same length of the short sides of the hexagons and semi-regular hexagons has sides of length 1 and $\frac{\sqrt{2}}{2}$. Naturally, this is not necessarily the representation corresponding to the same surface of R_1 , but keeping the ration of the two sides we can proportionally change the sizes of the sides to have the same surface. To find the new sizes we impose that the total area of the polygons appearing in R_2 must be the same of the total area of the polygons in R_1 provided it has all sides of length 1. A simple calculus shows that the area of the polygons in the first representation is

$$\mathcal{A}_1 = 2(2 + \sqrt{2})$$

and denoting by a and $a' = \frac{\sqrt{2}}{2}a$ the two side length in semi-regular hexagons the area of the second representation is

$$\mathcal{A}_2 = \sqrt{3}(1 + \sqrt{2})a.$$

We hence impose that $\mathcal{A}_1 = \mathcal{A}_2$ and obtain that the length of the sides in the semi-regular hexagon must be

$$a = \sqrt{\frac{2\sqrt{6}}{3}} \quad \text{and} \quad a' = \frac{\sqrt{2}}{2}a = \frac{\sqrt{2}}{2}\sqrt{\frac{2\sqrt{6}}{3}}.$$

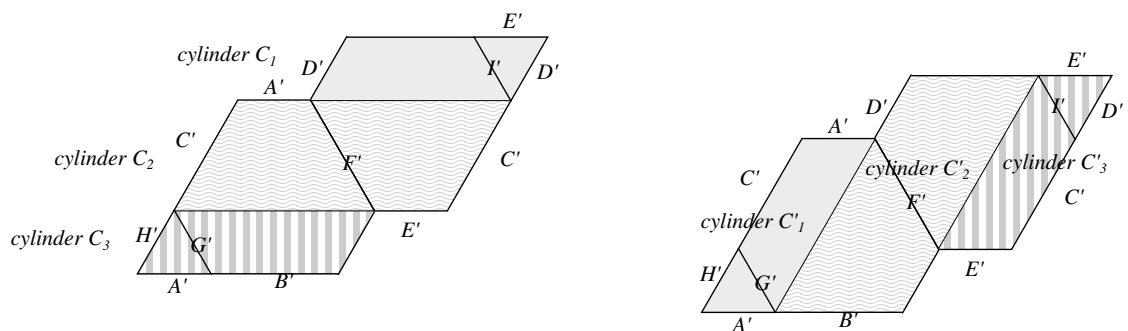


Figure 17: Second representation of $\mathcal{M}(3, 4)$.

3.2 Transition diagrams

Let us now consider a linear trajectory in the surface R_1 . Again, we can suppose that the trajectory does not hit any vertex and code such trajectory by recording the sides crossed by it considering the labelling given in Figure 13, obtaining a bi-infinite word in a new alphabet $\mathcal{A} = \{A, B, C, D, E, F, G, H\}$.

Again, we try to study the cutting sequence of the trajectory. Naturally, being each side of the squares glued to one in the octagon, it does not matter where we collocate the two squares with respect to the octagon as long as we preserve the glueing.

Since in this case the rotation of angle π does not preserve the labels, we have to consider trajectories in all directions in $[0, 2\pi]$. Sectors of total angle $\frac{\pi}{8}$ are the most natural for having the transitions in the cutting sequences determined and hence we divide the directions in 16 sectors of size $\frac{\pi}{8}$. For reasons that will become clear later on, we will call Σ_0 the sector $[\frac{7\pi}{8}, \pi]$ and enumerate the others clockwise so that $\Sigma_i = [\pi - \frac{(i+1)\pi}{8}, \pi - \frac{i\pi}{8}]$ for $i = 0, \dots, 15$. We have transformations of R_1 sending each Σ_i back in Σ_0 and preserving the figure and they are given by:

$$\begin{aligned} \nu_0 &= \text{Id}, & \nu_1 &= \rho_{-\frac{\pi}{8}} \circ r_1 \circ \rho_{\frac{\pi}{8}}, & \nu_2 &= \rho_{\frac{\pi}{4}}, & \nu_3 &= \rho_{-\frac{3\pi}{8}} \circ r_1 \circ \rho_{\frac{3\pi}{8}}, \\ \nu_4 &= \rho_{\frac{\pi}{2}}, & \nu_5 &= \rho_{\frac{\pi}{8}} \circ r_2 \circ \rho_{-\frac{\pi}{8}}, & \nu_6 &= \rho_{\frac{3\pi}{4}}, & \nu_7 &= r_2, \\ \nu_8 &= \nu_7 \circ r_1, & \nu_9 &= \nu_6 \circ r_1, & \nu_{10} &= \nu_5 \circ r_1, & \nu_{11} &= \nu_4 \circ r_1, \\ \nu_{12} &= \nu_3 \circ r_1, & \nu_{13} &= \nu_2 \circ r_1, & \nu_{14} &= \nu_1 \circ r_1, & \nu_{15} &= r_1. \end{aligned}$$

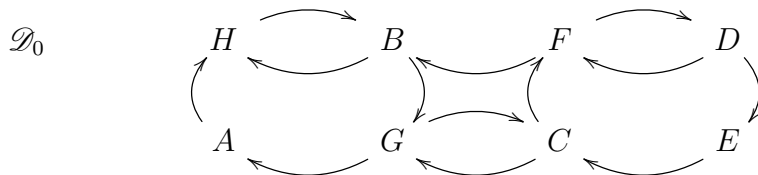
We recall that ρ_θ is the counter-clockwise rotation of angle θ and r_1 and r_2 are respectively the reflection with respect to the horizontal and vertical axis.

We computed the corresponding permutations and hence proved the following:

Lemma 3.1. *The permutations on the labels of R_1 corresponding by the action of the matrices above are*

$$\begin{aligned} \pi_0 &= \text{Id}, & \pi_1 &= (AD)(BC)(EH)(FG), \\ \pi_2 &= (ABCDEFGH), & \pi_3 &= (AC)(DH)(EG), \\ \pi_4 &= (ACEG)(BDFH), & \pi_5 &= (AB)(CH)(DG)(EF), \\ \pi_6 &= (ADGBEHCF), & \pi_7 &= (BH)(CG)(DF), \\ \pi_8 &= (AE)(BF)(CG)(DH), & \pi_9 &= (AH)(BG)(CF)(DE), \\ \pi_{10} &= (AFCHBEGD), & \pi_{11} &= (AG)(BF)(CE), \\ \pi_{12} &= (AGEC)(BHFD), & \pi_{13} &= (AF)(BE)(CD)(GH), \\ \pi_{14} &= (AHGFEDCB), & \pi_{15} &= (AE)(BD)(FH). \end{aligned}$$

We now investigate which transitions may occur in a cutting sequence by writing down the transition diagram corresponding to a trajectory in Σ_0 . The transition diagrams for trajectories in other directions would follow directly from this one by applying the corresponding permutations. The first transition diagram is:



We note that a cutting sequence in direction in Σ_i is a bi-infinite path in the corresponding transition diagram \mathcal{D}_i .

Remark 3.2. Given a trajectory τ in direction in Σ_i its normal form is the trajectory in direction in Σ_0

$$n(\tau) = \nu_k \tau.$$

Moreover, cutting sequences verify

$$c(n(\tau)) = \pi_k \cdot c(\tau).$$

3.3 Derivation

In this section we will prove a statement equivalent to Proposition 1.18 for the hexagon. We need hence to define some kind of combinatorial operation on words (the derivation) so that the derived sequence of a cutting sequence will be again a cutting sequence of another trajectory. Here we explain the role of the second representation: after deriving, we will effectively have the cutting sequence of another trajectory, but coded with respect to the sides of the second representation. This means that the derivation will be nothing else but the rule of how to pass from a cutting sequence in R_1 and the cutting sequence in R_2 after applying the matrix that sends R_1 to R_2 . To conclude the procedure and get a cutting sequence of a new trajectory in the same surface, we have to do the same procedure on R_2 .

As before, we have:

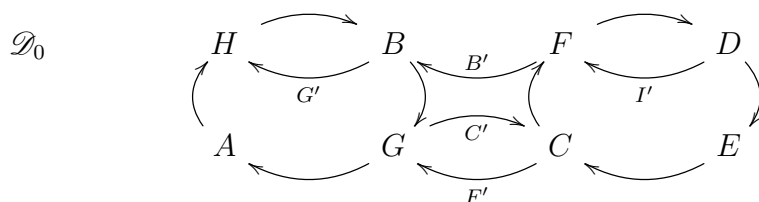
Definition 3.3. A word in the alphabet $w \in \mathcal{A}^{\mathbb{Z}}$ is admissible if it represents a bi-infinite path in one of the diagrams \mathcal{D}_i .

and by construction

Lemma 3.4. If $w \in \mathcal{A}^{\mathbb{Z}}$ is a cutting sequence, it is admissible in one of the diagrams \mathcal{D}_i .

Let us first define the derivation for sequences admissible in diagram \mathcal{D}_0 .

Definition 3.5. Let w be a word in $\mathcal{A}^{\mathbb{Z}}$ admissible in diagram \mathcal{D}_0 . Its derived sequence is the sequence in the new alphabet $\mathcal{A}' = \{A', B', C', D', E', F', G', H', I'\}$ obtained from w by interpolating it with the letters on the arrows of the following diagram, changing A, D, E, H with the correspondent primed and dropping letters B, C, F, G .



In a similar way we can define derivation on words admissible in the other diagrams.

3.4 Veech element

The main result that we have proved is the following:

Theorem 3.6. *Let us consider a trajectory τ in R_1 in direction $\theta \in \Sigma_0$ with cutting sequence $c(\tau)$. The derived sequence of the cutting sequence $c(\tau)$ is still a cutting sequence.*

We will now prove the theorem so that it describes how to pass from cutting sequences in one representation to cutting sequences in the other. We will hence find the deformations we need to apply to pass from one representation to the other.

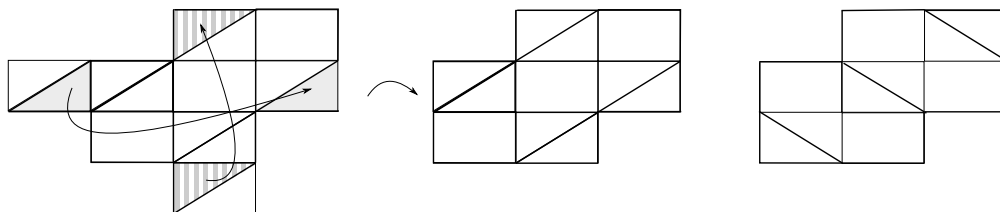


Figure 18: The representations R_1^\perp and R_2^\perp .

Proof. First step. The key observation for finding out how to go from one representation to the other is made by comparing the polygonal decompositions R_1^\perp and R_2^\perp , which were obtained from the graph as explained. As one can easily see looking at Figure 18, R_1^\perp and R_2^\perp are the same up to cutting and pasting two half rectangles, translation equivalence that we will call $\tilde{\Upsilon}_S$. We call its image \tilde{R}_1^\perp .

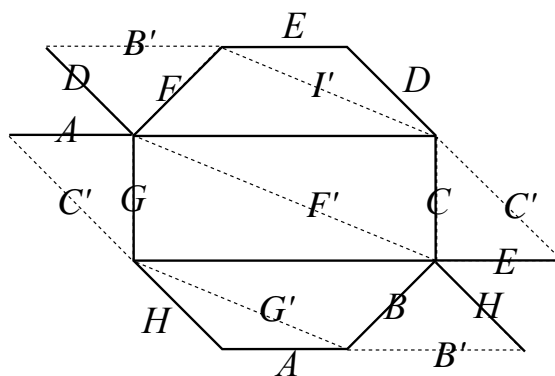


Figure 19: $\Upsilon_S R_1 = \tilde{R}_1$.

Naturally, we can apply the induced cut and paste to the representation R_1 and we will call this map Υ_S , obtaining a representation \tilde{R}_1 . We remark that this

map has in fact the same role as Υ_{S_E} in the previous section. Moreover, this figure allows us to see how R_2 can be obtained by shearing R_1 after applying Υ_S .

Second step. On cutting sequences, Υ act by adding some necessary sides that we will call auxiliary sides from now on (see Figure 19) and dropping some others. We can hence record in the diagram of admissible transitions the crossing of auxiliary sides. It is clear that some sides are shared from the two configurations, precisely A, D, E, H , some must be added and are the one on the augmented diagram (3.5) and some more must be eliminated, because they are not part of the sides of the new configuration, precisely B, C, F, G . This step is equivalent to the third step of the proof of the similar proposition for the hexagon, when we applied the cut and paste to the new hexagon and wrote the cutting sequence $\bar{c}(\tau)$ with respect to the new sides. It turned out to be, in fact, exactly the derived sequence of the original cutting sequence.

Third step. In the previous case the next step was to send the sheared hexagon back in the previous one, by applying a Veech element. In this case, we send the configuration \tilde{R}_1 to R_2 instead.

To send \tilde{R}_1 to R_2 , we apply three different transformations and consider their composition $\sigma = \sigma_3 \circ \sigma_2 \circ \sigma_1$.

- The first one, σ_1 will bring \tilde{R}_1 in R_2^\perp , easier to compare with R_2^\perp and hence with R_2 .

Since the two decompositions were in directions 0 and $\frac{3\pi}{4}$ we choose a shear to make them orthogonal, given by the matrix

$$\sigma_1 = \begin{pmatrix} 1 & 1 \\ 0 & 1 \end{pmatrix}.$$

- The second one in to adjust lengths and obtain from R_1^\perp the configuration R_2^\perp . We want it to act as in Figure 20 and hence we use the matrix:

$$\sigma_2 = \begin{pmatrix} \frac{\sqrt{2}}{2} \sqrt{\frac{2\sqrt{6}}{3}} & 0 \\ 0 & \frac{\sqrt{3}}{2} \sqrt{\frac{2\sqrt{6}}{3}} \end{pmatrix}.$$

- The third one will send R_2^\perp back in the original configuration R_2 . It hence sends vertical directions in the directions of the cylinder decompositions in R_2 corresponding to the ones in R_1 . Those decompositions are the ones in direction 0 and the one in direction $\frac{\pi}{3}$ as shown in Figure 17. The shear that sends vertical lines in lines in direction $\frac{\pi}{3}$ is:

$$\sigma_3 = \begin{pmatrix} 1 & \frac{\sqrt{3}}{3} \\ 0 & 1 \end{pmatrix}.$$

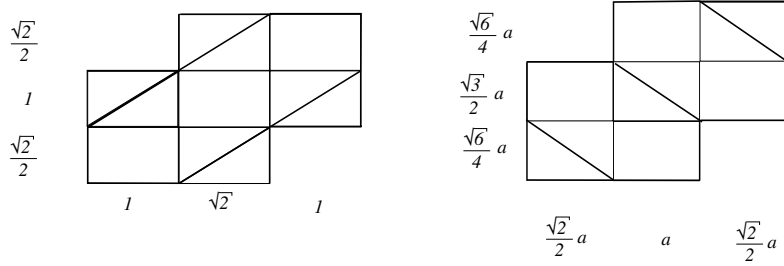


Figure 20: The lengths comparison between R_1^\perp and R_2^\perp .

Finally, we consider the composition of the three of them

$$\tilde{R}_1 \xrightarrow{\sigma_1} R_1^\perp \xrightarrow{\sigma_2} R_2^\perp \xrightarrow{\sigma_3} R_2$$

γ

which is given by the matrix

$$\sigma = \sigma_3 \circ \sigma_2 \circ \sigma_1 = \begin{pmatrix} \frac{\sqrt{2}}{2} \sqrt{\frac{2\sqrt{6}}{3}} & \frac{1}{2} \sqrt{\frac{2\sqrt{6}}{3}} (1 + \sqrt{2}) \\ 0 & \frac{\sqrt{3}}{2} \sqrt{\frac{2\sqrt{6}}{3}} \end{pmatrix}.$$

Geometrically, the action is showed in Figure 21.

$$R_1 \xrightarrow{\sigma_1} R_1^\perp \xrightarrow{\sigma_2} R_2^\perp \xrightarrow{\sigma_3} R_2$$

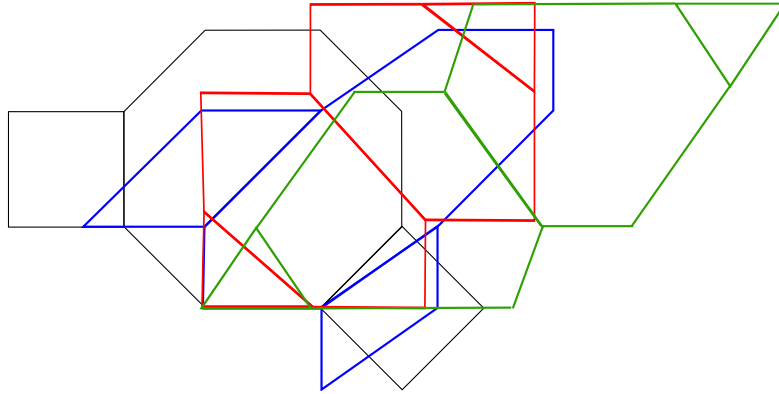


Figure 21: The action of σ .

Fourth step Since R_1 and R_2 represent the same surface this must be in the Veech group of it. As explained for the hexagon, we can consider the affine equivalence $\Psi_\sigma: S \rightarrow S$ obtained by the composition of $\Upsilon: S \rightarrow S$ and the deformation $\Phi_\sigma: S \rightarrow S$. Ψ_σ is the affine equivalence induced by the Veech element.

■

We actually proved something more precise than Theorem 3.6 that is the following proposition, similar to the one in Section 1.18:

Proposition 3.7. *Given a trajectory τ in R_1 in direction $\theta \in \Sigma_0$ with cutting sequence $c(\tau)$, let us consider the trajectory $\tau' = \Psi_\sigma \tau$ in R_2 . We have that the derived sequence of the original trajectory is the cutting sequence of the new trajectory. This means*

$$c(\tau') = c(\tau)'$$

The proof follows immediately from the last step of the proof of the theorem.

3.5 Future works

To obtain a complete characterization or at least a complete necessary condition, we need to do something more. The next step will be in fact to do the same thing for the configuration R_2 , finding out how to shear, scale and shear it again to obtain a sheared R_1 that can be sent back in the original configuration so that the procedure can start again and we can affirm that a cutting sequence is infinitely derivable, defining the derivation as alternating the one for R_1 and the one we will give for R_2 .

The idea we are following is to consider the symmetric cylinder decomposition in direction $\frac{2\pi}{3}$ in R_2 together with the horizontal one and apply the same procedure. The first thing is to shear R_2 so that the two cylinder decompositions become orthogonal. Then we are planning to modify lengths again to return to the configuration where the cylinder decompositions symmetric to the ones we considered until now in R_1 (which means, the horizontal one and the one in direction $\frac{\pi}{4}$) are orthogonal. Finally, we want to shear it again to a sheared representation R_1 .

Applying the correspondent matrices of the action we just explained gives a shear:

$$\begin{aligned} \gamma &= \begin{pmatrix} 1 & 1 \\ 0 & 1 \end{pmatrix} \begin{pmatrix} \sqrt{2}\sqrt{\frac{2\sqrt{6}}{3}} & 0 \\ 0 & \frac{2\sqrt{3}}{3}\sqrt{\frac{2\sqrt{6}}{3}} \end{pmatrix} \begin{pmatrix} 1 & \frac{\sqrt{3}}{3} \\ 0 & 1 \end{pmatrix} \\ &\cdot \begin{pmatrix} 1 & \frac{\sqrt{3}}{3} \\ 0 & 1 \end{pmatrix} \begin{pmatrix} \frac{\sqrt{2}}{2}\sqrt{\frac{2\sqrt{6}}{3}} & 0 \\ 0 & \frac{\sqrt{3}}{2}\sqrt{\frac{2\sqrt{6}}{3}} \end{pmatrix} \begin{pmatrix} 1 & 1 \\ 0 & 1 \end{pmatrix} = \begin{pmatrix} 1 & 2 + \sqrt{2} \\ 0 & 1 \end{pmatrix} \end{aligned}$$

which has as argument exactly the modulus of all the three cylinders in the horizontal decomposition. This is in fact the shear that Diana Davis is using in her works about Bouw-Möller surfaces. However, her method does not consider the two representations of Bouw-Möller surfaces and try to pass directly again to the same representation. In this way, she cannot cover all sectors of directions of trajectories. Even if our method seems to result a bit longer because we have

a intermediate step, each step turns out to be much easier passing for the second representations, more similar to the one used in [SU11] and more useful to understand what is happening in the Teichmüller disk of deformations.

The next step will be to find the position of the sides of the sheared R_2 and record them in the diagram of admissible transitions.

The reason for choosing the numeration of sectors as we did is that in this way, as we had in the previous cases, the natural range Σ_0 of directions for R_1 is sent in the new configuration in a bigger interval of directions: it is sent in $[\frac{2\pi}{3}, \pi]$ which is range double of the natural angle for this configuration, which is $\frac{\pi}{6}$, to have the transition diagram. We will hence need some way of normalizing the trajectory and send them back in the new Σ'_0 . In fact, for R_2 we will divide the range of possible directions $[0, 2\pi]$ in 12 intervals $\Sigma'_i = [\pi - \frac{(i+1)\pi}{6}, \pi - \frac{i\pi}{6}]$ for $i = 0, \dots, 11$ and trajectories in Σ_0 will be sent in trajectories either in Σ_0 or Σ_1 .

Other future plans are to write down the two equivalent of the Farey maps and describe how to apply the two alternating between them as we alternate configurations.

Moreover, it would be meaningful to try to find out what is happening in the Teichmüller disk while applying the matrices described before (naturally, all of them are in $SL(2, \mathbb{R})$ because they need to preserve areas). We would expect to have a tree equivalent to the one for the other case, but bipartite, with vertices with m edges and vertices with n edges corresponding to the different configurations.

Finally, we will try to understand how to generalize this method to a general Bouw-Möller surface.

References

- [BM10] Irene I. Bouw and Martin Möller. Teichmüller curves, triangle groups, and Lyapunov exponents. *Annals of Mathematics (2)*, 172(1):139–185, 2010.
- [Dav13] Diana Davis. Cutting sequences, regular polygons, and the Veech group. *Geometriae Dedicata*, 162:231–261, 2013.
- [Dav14] Diana Davis. Cutting sequences on bouw-möller surfaces. In preparation, 2014.
- [Hoo08] Patrick W. Hooper. The bouw-möller lattice surfaces and eigenvectors of grid graphs. 2008.
- [Hoo12] Patrick W. Hooper. Grid graphs on lattice surfaces. To appear in International Mathematics Research Notices, 2012.
- [HS06] Pascal Hubert and Thomas A. Schmidt. An introduction to Veech surfaces. In *Handbook of dynamical systems. Vol. 1B*, pages 501–526. Elsevier B. V., Amsterdam, 2006.
- [Mas06] Howard Masur. Ergodic theory of translation surfaces. In *Handbook of dynamical systems. Vol. 1B*, pages 527–547. Elsevier B. V., Amsterdam, 2006.
- [Ser82] Caroline Series. Non-Euclidean geometry, continued fractions, and ergodic theory. *The Mathematical Intelligencer*, 4(1):24–31, 1982.
- [Ser85a] Caroline Series. The geometry of Markoff numbers. *The Mathematical Intelligencer*, 7(3):20–29, 1985.
- [Ser85b] Caroline Series. The modular surface and continued fractions. *Journal of the London Mathematical Society (2)*, 31(1):69–80, 1985.
- [SU10] John Smillie and Corinna Ulcigrai. Geodesic flow on the Teichmüller disk of the regular octagon, cutting sequences and octagon continued fractions maps. In *Dynamical numbers—interplay between dynamical systems and number theory*, volume 532 of *Contemp. Math.*, pages 29–65. Amer. Math. Soc., Providence, RI, 2010.
- [SU11] John Smillie and Corinna Ulcigrai. Beyond Sturmian sequences: coding linear trajectories in the regular octagon. *Proceedings of the London Mathematical Society. Third Series*, 102(2):291–340, 2011.

- [Vee89] W. A. Veech. Teichmüller curves in moduli space, Eisenstein series and an application to triangular billiards. *Inventiones Mathematicae*, 97(3):553–583, 1989.